AD-A118 443 UNIVERSITY OF SOUTH FLORIDA TAMPA DEPT OF ELECTRICAL--ETC F/G 2/1
NONLINEAR REPRESENTATION AND PULSE TESTING OF COMMUNICATION SUB--ETC(U)
MAY 82 V K JAIN, A M BUSH F30602-78-C-0120
UNCLASSIFIED SS-39PULVOL RADC-TR-82-138 NL

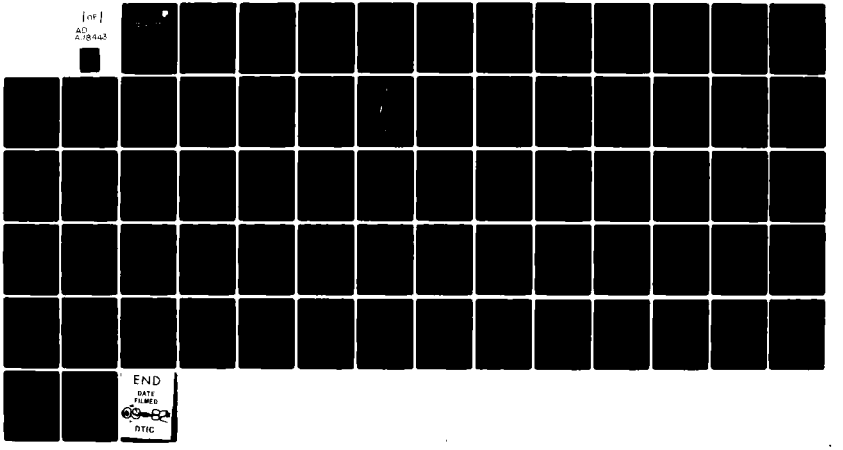

RADC-TR-82-138
Phase Report
May 1982

NONLINEAR REPRESENTATION AND PULSE TESTING OF COMMUNICATION SUBSYSTEMS

University of South Florida

Vijay K. Jain and Aubrey M. Bush

ROME AIR DEVELOPMENT CENTER
Air Force Systems Command
Griffiss Air Force Base, NY 13441

This report has been reviewed by the RADC Public Affairs Office (PA) and is releasable to the National Technical Information Service (NTIS). At NTIS it will be releasable to the general public, including foreign nations.

RADC-TR-82-138 has been reviewed and is approved for publication.

APPROVED: Daniel J. Kenneally

DANIEL J. KENNEALLY
Project Engineer

APPROVED: Edmund J. Westcott

EDMUND J. WESTCOTT
Technical Director
Reliability & Compatibility Division

FOR THE COMMANDER: John P. Huss

JOHN P. HUSS
Acting Chief, Plans Office

If your address has changed or if you wish to be removed from the RADC mailing list, or if the addressee is no longer employed by your organization, please notify RADC (RBCT) Griffiss AFB NY 13441. This will assist us in maintaining a current mailing list.

Do not return copies of this report unless contractual obligations or notices on a specific document requires that it be returned.

MISSION
of
Rome Air Development Center

RADC plans and executes research, development, test and selected acquisition programs in support of Command, Control Communications and Intelligence (C^3I) activities. Technical and engineering support within areas of technical competence is provided to ESD Program Offices (POs) and other ESD elements. The principal technical mission areas are communications, electromagnetic guidance and control, surveillance of ground and aerospace objects, intelligence data collection and handling, information system technology, ionospheric propagation, solid state sciences, microwave physics and electronic reliability, maintainability and compatibility.

UNCLASSIFIED

SECURITY CLASSIFICATION OF THIS PAGE (When Data Entered)

REPORT DOCUMENTATION PAGE		READ INSTRUCTIONS BEFORE COMPLETING FORM
1. REPORT NUMBER RADC-TR-82-138	2. GOVT ACCESSION NO. AD-A118 443	3. RECIPIENT'S CATALOG NUMBER
4. TITLE (and Subtitle) NONLINEAR REPRESENTATION AND PULSE TESTING OF COMMUNICATION SUBSYSTEMS		5. TYPE OF REPORT & PERIOD COVERED Phase Report 1 Nov 79 - 30 Sep 81
		6. PERFORMING ORG. REPORT NUMBER No. SS-39PULVOL
7. AUTHOR(s) Vijay K. Jain Aubrey M. Bush		8. CONTRACT OR GRANT NUMBER(s) F30602-78-C-0120
9. PERFORMING ORGANIZATION NAME AND ADDRESS Department of Electrical Engineering University of South Florida Tampa FL 33620		10. PROGRAM ELEMENT, PROJECT, TASK AREA & WORK UNIT NUMBERS 62702F 233803PN
11. CONTROLLING OFFICE NAME AND ADDRESS Rome Air Development Center (RBCT) Griffiss AFB NY 13441		12. REPORT DATE May 1982 13. NUMBER OF PAGES 59
14. MONITORING AGENCY NAME & ADDRESS(if different from Controlling Office) Same		15. SECURITY CLASS. (of this report) UNCLASSIFIED 15a. DECLASSIFICATION/DOWNGRADING SCHEDULE N/A

16. DISTRIBUTION STATEMENT (of this Report)

Approved for public release; distribution unlimited.

17. DISTRIBUTION STATEMENT (of the abstract entered in Block 20, if different from Report)

Same

18. SUPPLEMENTARY NOTES

RADC Project Engineer: Daniel J. Kenneally (RBCT)

19. KEY WORDS (Continue on reverse side if necessary and identify by block number)

Nonlinear systems	Pencil-of-functions	Simulation
Volterra series	Gram matrix	Digital response
Nonlinear transfer functions	Pulse input	Intermodulation distortion
Black-box modeling	Volterra Kernel identification	Interference

20. ABSTRACT (Continue on reverse side if necessary and identify by block number)

In this report we describe a method for determining the linear and quadratic subsystems from square-pulse tests. The identification method involves two transient test in the laboratory, followed by analysis by the computer. Advantages of the method include the rapidity of the laboratory tests, as contrasted with traditional frequency-scan approaches, and the explicit determination of the transfer functions. Furthermore, the method is also extendible to $H_3(s_1,s_2,s_3)$.

DD FORM 1 JAN 73 1473 EDITION OF 1 NOV 65 IS OBSOLETE

UNCLASSIFIED

SECURITY CLASSIFICATION OF THIS PAGE (When Data Entered)

ACKNOWLEDGEMENTS

The authors are deeply indebted to Mr. D. J. Kenneally and Mr. John F. Spina for their assistance and constructive criticism throughout this project. They wish to thank Dr. M. R. Donaldson for his encouragement to pursue this research and Dr. Donald D. Weiner for the many helpful discussions. Also, sincere thanks are due to Mr. Jacob Scherer of the Post Doc program for his interest and helpfulness.

The authors also acknowledge the assistance of Randy L. Colvin in making computer runs.

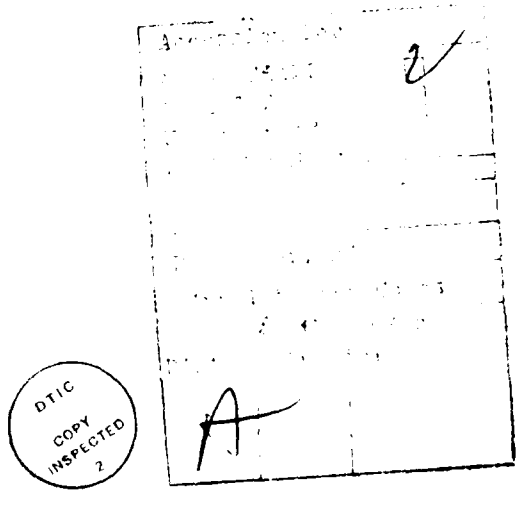

PREFACE

This effort was conducted by University of South Florida under the sponsorship of the Rome Air Development Center Post-Doctoral Program for Rome Air Development Center. Mr. D. J. Kenneally RADC/RBCT was the task project engineer and provided overall technical direction and guidance.

The RADC Post-Doctoral Program is a cooperative venture between RADC and some sixty-five universities eligible to participate in the program. Syracuse University (Department of Electrical Engineering), Georgia Institute of Technology (School of Electrical Engineering), University of Kansas (Department of Electrical Engineering), University of South Florida (Department of Electrical Engineering) and SCEEE, Inc. act as prime contractor schools with other schools participating via sub-contracts with prime schools. The U. S. Air Force Academy (Department of Electrical Engieering), Air Force Institute of Technology (Department of Electrical Engineering), and the Naval Post Graduate School (Department of Electrical Engineering) also participate in the program.

The Post-Doctoral Program provides an opportunity for faculty at participating universities to spend up to one year full time on exploratory development and problem-solving efforts with the post-doctorals splitting their time between the customer location and their educational institutions. The program is totally customer-funded with current projects being undertaken for Rome Air Development Center (RADC), Space and Missile Systems Organization (SAMSO), Aeronautical System Division (ASD), Electronics Systems Division (ESD), Air Force Avionics Laboratory (AFAL), Foreign Technology Division (FTD), Air Force Weapons Laboratory (AFWL), Armament Development and Test Center (ADTC), Air Force Communications Service (AFCS), Aerospace Defense Command (ADC), HW USAF, Defense Communications Agency (DCA), Navy, Army, Aerospace Medical Division (AMD), and Federal Aviation Administration (FAA).

Further information about the RADC-Doctoral Program can be obtained from Mr. Jacob Scherer, RADC/RBC, Griffis AFB, NY, 13441, telephone Autovon 587-4109, Commercial (315) 330-4109.

TABLE OF CONTENTS

LIST OF FIGURES

I. INTRODUCTION

In strategic communication systems the multiplicity of transmitters and receivers produces a large ensemble of interference sources that must be carefully examined both during the design and testing phases. To complicate matters further, the link between the ith transmitter and the jth receiver can exhibit nonlinear characteristics, thereby generating intermodulation and cross-modulation effects. These intermodulation and crossmodulation products can often increase to intolerable high levels, due to accumulation of distortion along the link. Reduction, then, must be achieved through compensation, or redesign of certain subsystems. Clearly, in testing such communication systems it is important to make certain that the nonlinear distortion lies within acceptable limits. The Volterra series expansion [1]-[3] permits description of a nonlinear system in a compact form and, in turn, enables computation of the distortion in terms of the multivariable transfer functions [4]-[6].

To date, however, reliable and rapid methods for finding the Volterra transfer functions (or kernels) from laboratory tests have been lacking. The work by Schetzen requires the use of wideband random excitation [7], which is somewhat impractical in a laboratory environment, both because suitable wideband sources with guaranteed uniform spectral density in the region of interest are difficult to find and, because their digital analysis requires unduly high sampling rates. Further, the method requires sufficient statistical averaging, involving guesswork on the part of the test engineer. The method by Weiner and Ewen [8] uses deterministic input, but they assume a rather restrictive model, namely with linear transfer function $H_1(s)$ and quadratic transfer function $H_2(s_1,s_2)=\beta H_1(s_1)H_1(s_2)H_1(s_1+s_2)$, where '$\beta$' is a gain constant. In realistic systems, the modes and frequencies, as well as the residues, of the quadratic subsystem may be different from those suggested by this model. Further, the test input they use is an exponentially decaying signal, not readily available from standard signal sources.

In this report we describe a method for determining the linear and quadratic subsystems from square-pulse tests. The quadratic subsystem is

assumed to be symmetric, but of the form $H_2(s_1,s_2)=H_a(s_1)H_a(s_2)H_c(s_1+s_2)$ so that it permits sufficient generality. The identification method involves two transient test in the laboratory, followed by analysis by the computer. The latter consists of (a) pole determination using the pencil-of-functions method [9]-[12] and (b) computation of the residues by a least-squares technique. Advantages of the method include the rapidity of the laboratory tests, as contrasted with traditional frequency-scan approaches, and the explicit determination of the transfer functions. Furthermore, the method is readily extendible to $H_3(s_1,s_2,s_3)$ and even to higher order transfer functions, although the computations grow very rapidly for these cases. The identification technique developed here represents a significant improvement over existing identification techniques, and is potentially a way to turn-key automatic test systems.

The structure of the report is as follows. In Section II we study the z-domain representation of quadratic Volterra subsystem. Section III discusses a general method for computation of the response of the linear and the quadratic subsystems. In Section IV the bilinear and Volterra responses of the quadratic subsystem to square pulses is computed in the form of explicit formulas. The form of the responses shows they are representable as the step, or impulse responses of certain equivalent linear systems.

As a consequence, the pencil-of-functions method by Jain[10]-[12] can be used to determine the poles of the quadratic subsystem. The complete identification procedure for a two-variable system is discussed in Section V. Computer generated examples, also presented in Section V, demonstrate the success of the approach developed in this report.

II. z-DOMAIN CHARACTERIZATION OF THE QUADRATIC VOLTERRA SYSTEM

In this section we shall be interested in the z-domain characterization of the quadratic nonlinear system shown in Fig. 1. This system is the most basic quadratic Volterra system, henceforth referred to as the single multiplier (1M) configuration. It will be shown that this system can be represented mathematically by the second degree term in the Volterra series [14], [7] with the corresponding quadratic transfer function $H_2(s_1, s_2) = H_a(s_1) H_b(s_2) H_c(s_1 + s_2)$. For the case where H_a, H_b and H_c are rational, we will find the z-domain description of this system for impulse and step invariant criteria. Throughout we will assume these components are causal and linear.

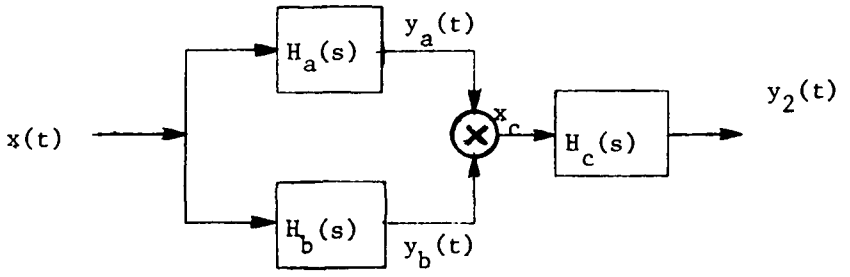

Fig. 1. Basic quadratic Volterra system

2.1 Continuous-Time Analysis

From Fig. 1 we observe the output of the multiplier to be

$$x_c(t) = \int_{-\infty}^{\infty} h_a(\xi)\, x(t-\xi)\, d\xi \int_{-\infty}^{\infty} h_b(\eta)\, x(t-\eta)\, d\eta \qquad (1)$$

From this the response of block H_c, i.e., the system output, is found to be

$$y_2(t) = \int_{-\infty}^{\infty} h_c(\tau)\, x_c(t-\tau)\, d\tau$$

$$= \int_{-\infty}^{\infty} h_c(\tau) \int_{-\infty}^{\infty} h_a(\xi)\, x(t-\tau-\xi)\, d\xi \int_{-\infty}^{\infty} h_b(\eta)\, x(t-\tau-\eta)\, d\eta\, d\tau \qquad (2)$$

Letting $\tau_1 = \tau + \xi$, and $\tau_2 = \tau + \eta$, we have

$$y_2(t) = \int_{-\infty}^{\infty}\int\int h_c(\tau)\, h_a(\tau_1-\tau)\, h_b(\tau_2-\tau)\, x(t-\tau_1)\, x(t-\tau_2)\, d\tau_1\, d\tau_2\, d\tau$$

$$= \int_{-\infty}^{\infty}\int\int h_2(\tau_1,\tau_2)\, x(t-\tau_1)\, x(t-\tau_2)\, d\tau_1\, d\tau_2 \qquad (3)$$

where

$$h_2(\tau_1,\tau_2) = \int_{-\infty}^{\infty} h_c(\tau)\, h_a(\tau_1-\tau)\, h_b(\tau_2-\tau)\, d\tau \qquad (4)$$

The two-dimensional Laplace-transform of h_2 is

$$H_2(s_1,s_2) = \int_{-\infty}^{\infty}\int\int h_c(\tau)\, h_a(\tau_1-\tau)\, h_b(\tau_2-\tau)\, e^{-(s_1\tau_1+ s_2\tau_2)}\, d\tau_1\, d\tau_2\, d\tau$$

$$= \int_{-\infty}^{\infty} h_c(\tau)\, e^{-(s_1+ s_2)\tau} \int_{-\infty}^{\infty} h_a(\tau_1- \tau)\, e^{-s_1(\tau_1- \tau)}\, d\tau_1 \cdot$$

$$\int_{-\infty}^{\infty} h_b(\tau_2- \tau)\, e^{-s_2(\tau_2- \tau)}\, d\tau_2\, d\tau$$

$$= H_a(s_1)H_b(s_2)H_c(s_1+ s_2)$$

We will omit the qualifier "two-dimensional" when it is clear from the context. However, the significance of this qualifier becomes particularly evident when we associate with $y_2(t)$ in (3) the following two-dimensional response

$$\bar{y}_2(t_1,t_2) = \int_{-\infty}^{\infty}\int\int h_2(\tau_1,\tau_2)\, x(t_1- \tau_1)\, x(t_2- \tau_2)\, d\tau_1\, d\tau_2 \qquad (6)$$

Straightforward application of the definition of two-dimensional Laplace transform and some manipulation, yields

$$\bar{Y}_2(s_1, s_2) = H_2(s_1, s_2)\, X(s_1)\, X(s_2) \tag{7a}$$

$$= H_2(s_1, s_2)\, \bar{X}(s_1, s_2) \tag{7b}$$

which represents the input-output relationship of a two-dimensional linear system as shown in Fig. 2. We will call $\bar{y}_2(t_1, t_2)$ the associated two-dimensional response since $y_2(t) = \bar{y}_2(t_1, t_2)\Big|_{t_1=t_2=t}$

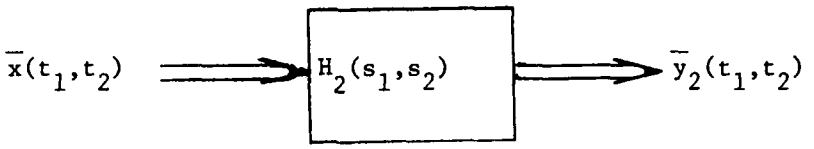

Fig. 2. Associated two-dimensional linear system

Rational Case

When

$$H_a = \sum_{i=1}^{n} \frac{A_i}{s+a_i}$$

$$H_b = \sum_{j=1}^{n} \frac{B_j}{s+b_j} \tag{8a}$$

$$H_c = \sum_{\ell=1}^{n} \frac{C_\ell}{s+c_\ell}$$

or, equivalently,

$$h_a(t) = \sum_{i=1}^{n} A_i\, e^{-a_i t}$$

$$h_b(t) = \sum_{j=1}^{n} B_j\, e^{-b_j t} \qquad t \geq 0 \tag{8b}$$

$$h_c(t) = \sum_{\ell=1}^{n} C_\ell\, e^{-c_\ell t}$$

then equations (3), (6) and (7) may be written as

$$y_2(t) = \sum_{i,j,\ell=1}^{n} A_i B_j C_\ell \iint_{-\infty}^{\infty} g_{ij\ell}(\tau_1,\tau_2)\, x(t-\tau_1)\, x(t-\tau_2)\, d\tau_1\, d\tau_2 \qquad (9a)$$

$$\bar{y}_2(t_1,t_2) = \sum_{i,j,\ell=1}^{n} A_i B_j C_\ell \iint_{\infty}^{\infty} g_{ij\ell}(\tau_1,\tau_2)\, x(t_1-\tau_1)\, x(t_2-\tau_2)\, d\tau_1\, d\tau_2 \qquad (9b)$$

$$\bar{Y}_2(s_1,s_2) = \sum_{i,j,\ell=1}^{n} A_i B_j C_\ell \quad G_{ij\ell}(s_1,s_2)\, \bar{X}(s_1,s_2) \qquad (9c)$$

where

$$G_{ij\ell}(s_1,s_2) = \frac{1}{(s_1+a_i)(s_2+b_j)(s_1+s_2+c_\ell)} \qquad (10a)$$

$$g_{ij\ell}(\tau_1,\tau_2) = \mathcal{L}^{-1}\, G_{ij\ell}(s_1,s_2) \qquad (10b)$$

It follows from (9)-(10) that the response is a weighted triple sum over the response of the elementary quadratic system shown in Fig. 3 where $a = a_i$, $b = b_j$, and $c = c_\ell$. We will abbreviate this process of triple summation as WTS. Thus, we arrive at the important conclusion that it is only necessary to analyze the elementary system of Fig. 3 in detail; the properties of the original system, e.g., its response, would follow immediately through the appropriate WTS process.

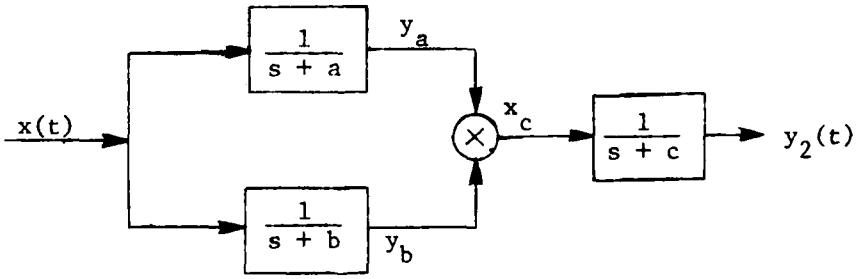

Fig. 3. Elementary quadratic system

Impulse response of the elementary quadratic system

Using $h_\alpha(t) = e^{-\alpha t}\, u(t)$, $\alpha = a,b,c$ in equation (4) we obtain the quadratic

Volterra kernel for the elementary system of Fig. 3 as

$$g(\tau_1,\tau_2) = \int_{-\infty}^{\infty} e^{-c\tau} u(\tau)\, e^{-a(\tau_1-\tau)}\, u(\tau_1-\tau)\, e^{-b(\tau_2-\tau)}\, u(\tau_2-\tau)\, d\tau$$

$$= \int_{0}^{\tau^*} e^{-(c-a-b)\tau}\, d\tau\; u(\tau^*)\, e^{-a\tau_1}\, e^{-b\tau_2}$$

$$= e^{-a\tau_1}\, e^{-b\tau_2}\, \frac{1 - e^{-(c-a-b)\tau^*}}{c-a-b}\, u(\tau_1)\, u(\tau_2) \qquad (11)$$

where[1] $\tau^* = \text{Min}(\tau_1, \tau_2)$, it is assumed that $c \neq a + b$.

The impulse response of the elementary quadratic system is obtained by setting $\tau_1 = \tau_2 = t$ in (11):

$$y_2(t) = \frac{e^{-(a+b)t} - e^{-ct}}{c - a - b}\, u(t) \qquad (12)$$

Example 1

For $a = 1$, $b = 3$ and $c = 6$ we have

$$g(\tau_1,\tau_2) = e^{-\tau_1 - 3\tau_2}\, \frac{1 - e^{-2\tau^*}}{2}\, u(\tau_1)\, u(\tau_2)$$

This is depicted in Fig. 4 where the hatched region denotes the region of zero value for $g(\tau_1,\tau_2)$.

Note also that the two-dimensional response to the input

$$\bar{x}(t_1,t_2) = \delta(t_1-\alpha)\, \delta(t_2-\beta)$$

is

$$\bar{y}_2(t_1,t_2) = e^{-a(t_1-\alpha)}\, e^{-b(t_2-\beta)}\, \frac{1 - e^{-(c-a-b)t^*}}{c-a-b} \cdot u(t_1-\alpha)\, u(t_2-\beta)$$

[1] The upper limit τ^* implies that integration is done from 0 to τ_1 or τ_2, whichever is smaller.

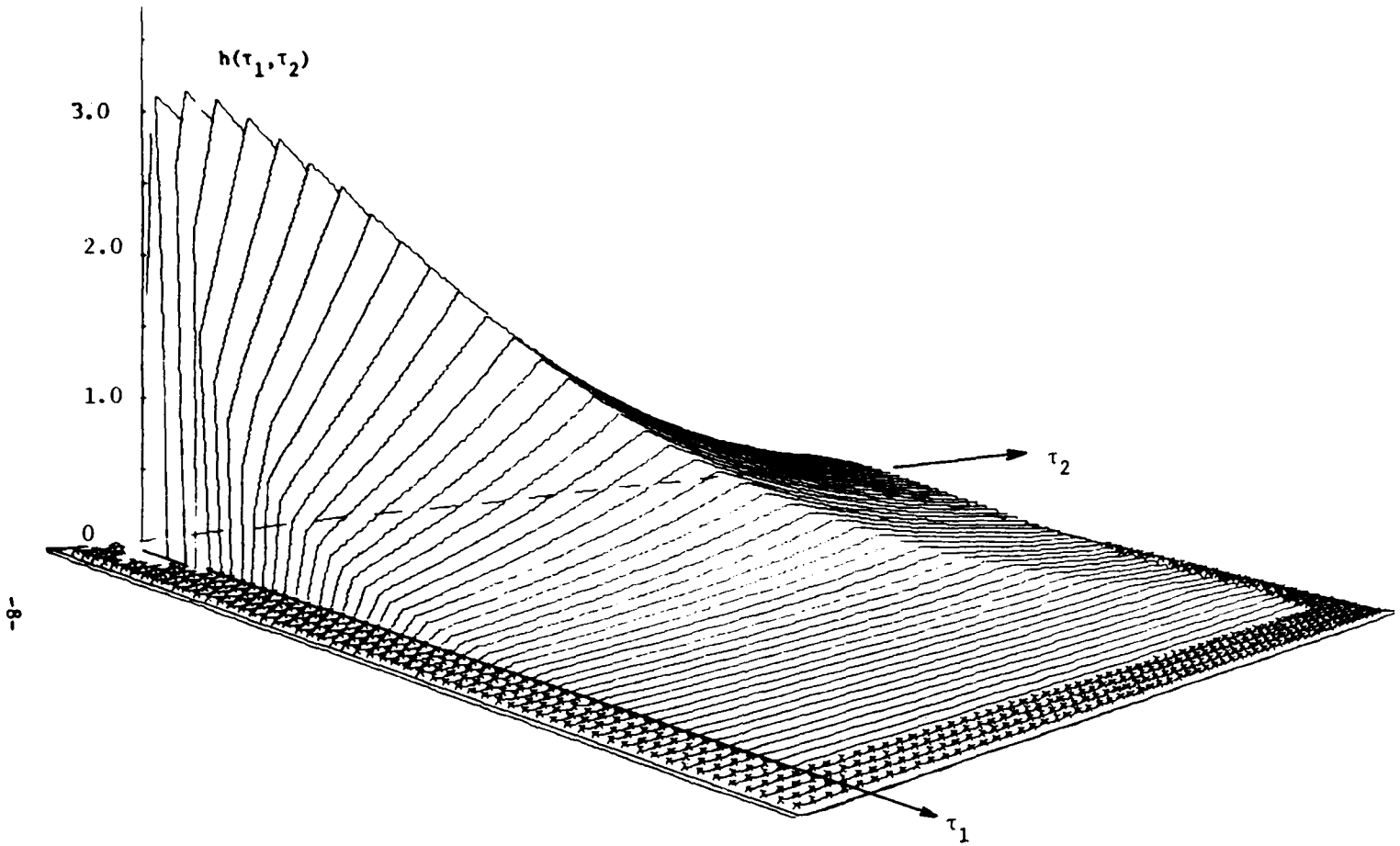

EXAMPLE ONE

AZIMUTH - 45 ALTITUDE - 20
*WIDTH - 10 *HEIGHT - 4.0

Fig. 4. A typical quadratic Kernel

where $t^* = \min \{t_1 - \alpha, t_2 - \beta\}$. This follows from (11) and the "stationarity" of the associated two dimensional system.

Bilinear Operator [7]

Equation (3) may be rewritten as

$$y_2(t) = V_2[x(t)]$$

$$= \int_{-\infty}^{\infty}\int h_2(\tau_1,\tau_2)\, x(t-\tau_1)\, x(t-\tau_2)\, d\tau_1\, d\tau_2$$

That is $y_2(t)$ may be viewed as the result of a nonlinear operator upon the input signal x(t). This operator may be generalized as

$$V_2\{x_1(t), x_2(t)\} = \int_{-\infty}^{\infty}\int h_2(\tau_1,\tau_2)\, x_1(t-\tau_1)\, x_2(t-\tau_2)\, d\tau_1\, d\tau_2 \qquad (13)$$

Clearly, $V_2\{.,.\}$ is bilinear in x_1 and x_2; we will call it the bilinear Volterra operator, or simply the bilinear operator. Note that

$$V_2[\, x\,] = V_2\{x, x\}$$

The significance of the bilinear operator arises from the fact that

$$V_2\Big[\sum_{i=1}^{n} a_i x_i\Big] = \sum_{i=1}^{n}\sum_{j=1}^{n} a_i a_j\, V_2\{x_i, x_j\} \qquad (14)$$

Example 2(a)

We will find the bilinear response of the elementary system of Fig. 3 for the case

$$x_1(t) = \delta(t-\alpha),\ x_2(t) = \delta(t-\beta)$$

where we will assume $\alpha \leq \beta$.

From equation (15) we find the bilinear response to be the convolution of $h_2(t_1,t_2)$ and $\delta(t_1-\alpha,\ t_2-\beta)$, with t_1 and t_2 set equal to t. This is equivalent to the integral of the product of $h_2(\tau_1,\tau_2)$ and a two-dimensional impulse located at $\tau_1 = t - \alpha$ and $\tau_2 = t - \beta$. This is depicted in Fig. 5a for four different values of t, namely $t = 0, \alpha, \beta$ and $t > \beta$. Now, for the particular case of the 1 - M system of Fig. 3, we have (denoting $1/(c-a-b)$ as ϕ)

$$V_2\{x_1,\ x_2\} = \int_0^\infty \int_0^{\tau_1} e^{-a\tau_1}\, e^{-b\tau_2}\, \frac{1-e^{-(c-a-b)\tau_2}}{c-a-b} \cdot$$

$$u(\tau_2)\ \delta(t-\beta-\tau_2)\ d\tau_2\ u(\tau_1)\ \delta(t-\alpha-\tau_1)\ d\tau_1$$

$$= \phi \int_0^\infty e^{-a\tau_1}\ \delta(t-\alpha-\tau_1) \int_0^{\tau_1} [e^{-b\tau_2} - e^{-(c-a)\tau_2}]\ \delta(t-\beta-\tau_2)\, d\tau_2\ d\tau_1$$

$$= \phi \int_0^\infty e^{-a\tau_1}\ \delta(t-\alpha-\tau_1)\, [e^{-b(t-\beta)} - e^{-(c-a)(t-\beta)}]\ u(\tau_1-t+\beta)\, d\tau_1$$

$$= \phi\ [e^{-b(t-\beta)} - e^{-(c-a)(t-\beta)}] \int_{t-\beta}^\infty e^{-a\tau_1}\ \delta(t-\alpha-\tau_1)\, d\tau_1\ u(t-\beta)$$

$$= \phi\ e^{-a(t-\alpha)} [e^{-b(t-\beta)} - e^{-(c-a)(t-\beta)}]\ u(t-\alpha)\ u(t-\beta)$$

$$= \frac{1}{c-a-b}\ e^{-a(t-\alpha)} [e^{-b(t-\beta)} - e^{-(c-a)(t-\beta)}]\ u(t-\beta)$$

For clarification of limits of integrations leading to steps two and three see Fig. 5b. A similar formula can be derived for the case $\alpha > \beta$.

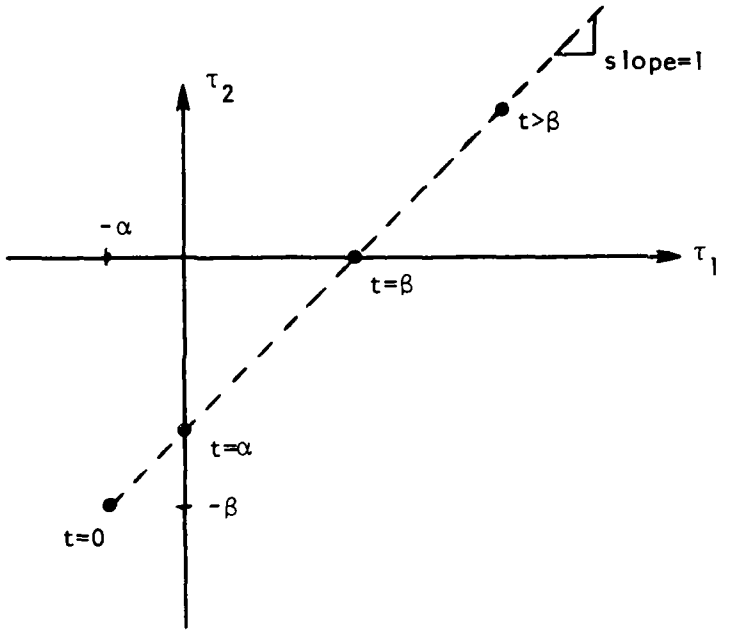

Fig. 5a. Location of two-dimensional impulse in the τ_1 - τ_2 plane.

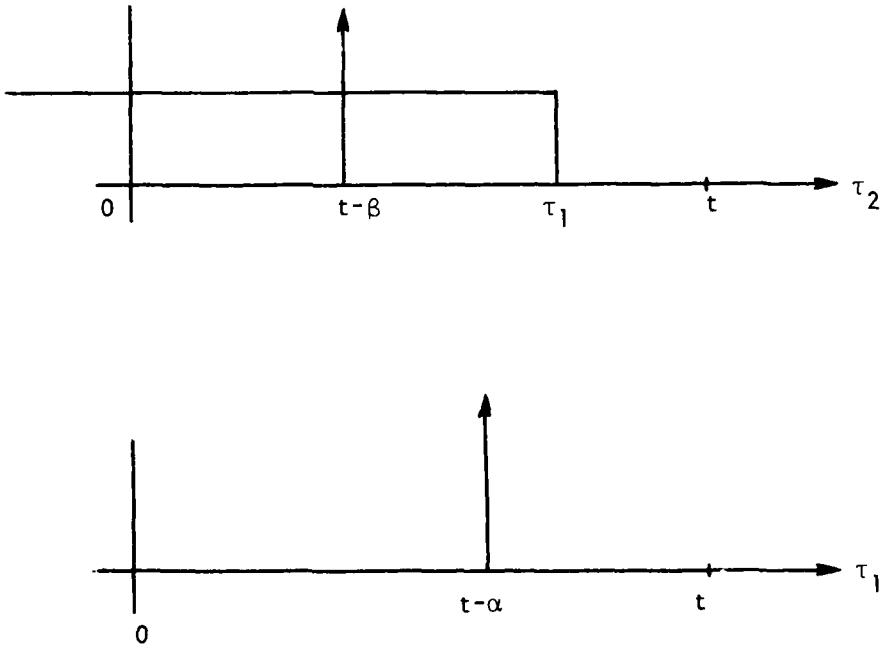

Fig. 5b. Limits of integration in Example 2

Note that the transform of $V_2\{x_1,x_2\}$ is

$$V_2\{X_1(s),\ X_2(s)\} = H_2(s_1,s_2)X_1(s_1)X_2(s_2) \tag{15}$$

and, clearly, (15) can also be written in the transform domain:

$$V_2[\sum_{i=1}^{n} a_i\ X_i(s)] = \sum_{i=1}^{n}\sum_{j=1}^{n} a_i a_j\ V_2\{X_i(s),\ X_j(s)\} \tag{16}$$

To demonstrate the usefulness of the transform domain we consider Example 2(a) again.

Example 2(b)

Since

$$X_1(s_1) = e^{-\alpha s_1}, \qquad X_2(s_2) = e^{-\beta s_2}$$

then

$$V_2\{X_1,X_2\} = \frac{1}{(s_1+a)(s_2+b)(s_1+s_2+c)}\ e^{-\alpha s_1}\ e^{-\beta s_2}$$

Application of George's theorem (Corollary-Appendix A) gives immediately the same time domain bilinear response as before.

Finally, before leaving the discussion on bilinear response, we note that the bilinear response of the general 1-M section with H_a, H_b, and H_c characterized by (8), is

$$V_2\{X_1,X_2\} = \sum_{i,j,\ell=1}^{n} A_i B_j C_\ell\ G_{ij\ell}(s_1,s_2)\ X_1(s_1)X_2(s_2) \tag{17}$$

The time-domain response is of course the inverse transform of (17).

Bilinear Response From Block Diagram -

We will show that the bilinear response of the 1-M (Fig. 1) section can be obtained by applying $x_1(t)$ to $H_a(s)$ and $x_2(t)$ to $H_b(s)$ as shown in Fig. 6(b). Of course, this procedure is useful only for pencil-and-paper purposes and simulation; it is not useful for practical situations where it is generally not possible to isolate $H_a(s)$ and $H_b(s)$.

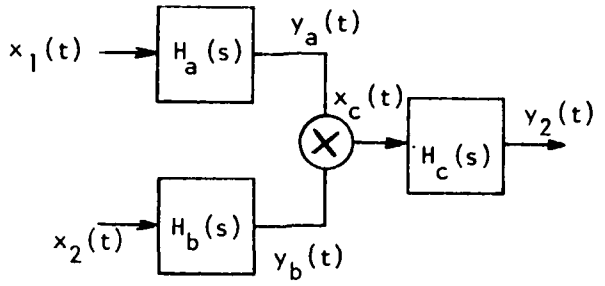

(a) Block-diagram for bilinear response

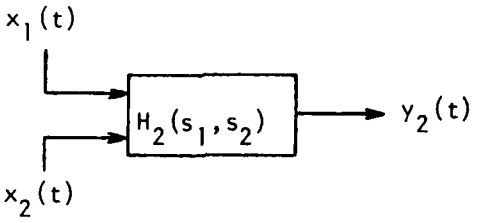

(b) Symbolic representation of bilinear response

Fig. 6. Bilinear response from block diagram

Substituting for $h_2(\tau_1,\tau_2)$ from (4) and interchanging the order of integration, we have

$$V_2\{x_1,x_2\} = \int_{\tau=-\infty}^{\infty} h_c(\tau) \int_{-\infty}^{\infty} h_a(\tau_1-\tau)x_1(t-\tau_1)d\tau_1 \int_{-\infty}^{\infty} h_b(\tau_2-\tau)x_2(t-\tau_2)d\tau_2 d\tau$$

or, with $\xi_1 = \tau_1 - \tau$ and $\xi_2 = \tau_2 - \tau$,

$$V_2\{x_1,x_2\} = \int_{\tau=-\infty}^{\infty} h_c(\tau) \int_{-\infty}^{\infty} h_a(\xi_1)x_1(t-\tau-\xi_1)d\xi_1 \int_{-\infty}^{\infty} h_b(\xi_2)x_2(t-\tau-\xi_2)d\xi_2 \, d\tau$$

$$= \int_{-\infty}^{\infty} h_c(\tau)\, y_a(t-\tau)\, y_b(t-\tau)\, dt$$

$$= \int_{-\infty}^{\infty} h_c(\tau)\, x_c(t-\tau)\, d\tau$$

where $y_a(t)$ is the response of $H_a(s)$ to the input $x_1(t)$, $y_b(t)$ the response of $H_b(s)$ to the input $x_2(t)$, and $x_c(t) = y_a(t)y_b(t)$. Therefore, the interpretation of (15) in the form of Fig. 6(a), and Fig. 6(b), is justified.

2.2 Impulse-Invariant z-Transform for 1-M Section

The concept of impulse invariance of a two-dimensional linear system can be enunciated as follows. Given that a continuous input signal $\bar{x}(t_1, t_2)$ is applied to the sampled-data system of Fig. 7a; then the system of Fig. 7b is said to be impulse-invariant if its response $y(k_1, k_2)$ to the sequence $\bar{x}(k_1, k_2) = \bar{x}(k_1\Delta, k_2\Delta)$ equals the sampled response $\bar{y}(k_1\Delta, k_2\Delta)$ of Fig. 7a.

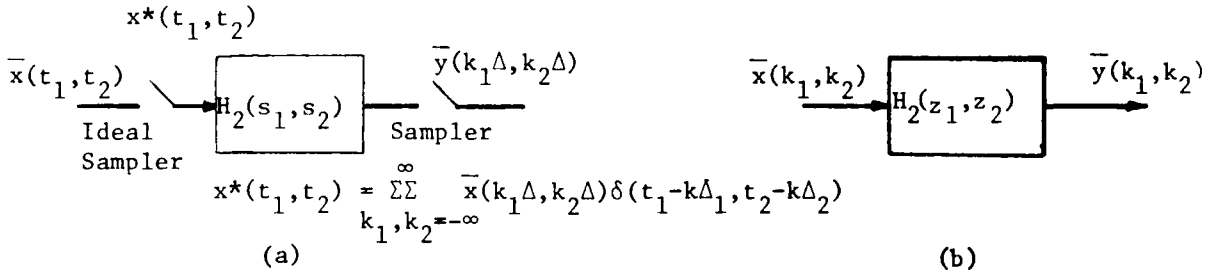

Fig. 7. Impulse invariant discrete-time system

Note that the above concept of impulse-invariance is a direct extension of this concept for the one-dimensional case [13].

We will use the known result that the impulse invariant equivalent z-domain function is given by the formula [14]

$$F(z_1,z_2)\Big|_{z_i = e^{s_i\Delta}} = \left(\frac{1}{2\pi j}\right)^2 \int_{-j\infty}^{+j\infty}\int \frac{F(v_1,v_2)\, dv_1\, dv_2}{(1-e^{-(s_1-v_1)\Delta})(1-e^{-(s_2-v_2)\Delta})} \qquad (18)$$

Specifically, for the function $G(s_1,s_2) = 1/(s_1+ a)(s_2+ b)(s_1+ s_2+ c)$, the quadratic transfer function of Fig. 3, we have

$$G(z_1, z_2)\Big|_{z_i=e^{s_i\Delta}} = \left(\frac{1}{2\pi j}\right)^2 \int_{-j\infty}^{j\infty}\int \frac{dv_1\, dv_2}{(v_1+a)(v_2+b)(v_1+v_2+c)(1-e^{-(s_1-v_1)\Delta})(1-e^{-(s_2-v_2)\Delta})}$$

$$= \left(\frac{1}{2\pi j}\right) \int_{-j\infty}^{j\infty} \frac{dv_2}{(v_2+b)(1-e^{-(s_2-v_2)\Delta})} \left[\frac{1}{(v_2+c-a)} \frac{1}{1-e^{-(s_1+a)\Delta}} - \frac{1}{1-e^{-(s_1+v_2+c)\Delta}}\right]$$

$$= \frac{e^{-(s_1+a)\Delta}}{1-e^{-(s_1+a)\Delta}} \frac{1}{2\pi j} \int_{-j\infty}^{j\infty} \frac{1}{(v_2+b)(v_2+c-a)(1-e^{-(s_2-v_2)\Delta})} \frac{1-e^{-(v_2+c-a)\Delta}}{(1-e^{-(s_1+v_2+c)\Delta})}\, dv_2$$

$$= \frac{e^{-(s_1+a)\Delta}}{1-e^{-(s_1+a)\Delta}} \frac{1}{2\pi j} \int_{-j\infty}^{j\infty} \frac{1-e^{-(v_2+c-a)\Delta}}{(v_2+b)(v_2+c-a)(1-e^{-(s_1+v_2+c)\Delta})} \frac{dv_2}{(1-e^{-(s_2-v_2)\Delta})}$$

$$= \frac{e^{-(s_1+a)\Delta}}{1-e^{-(s_1+a)\Delta}} \sum_{m=-\infty}^{\infty} \frac{1}{\Delta}\, Q(s_2 + j\,\frac{2\pi m}{\Delta})$$

$$= \frac{e^{-(s_1+a)\Delta}}{(1-e^{-(s_1+a)\Delta})(1-e^{-(s_1+s_2+c)\Delta})} \sum_{m=-\infty}^{\infty} \frac{1}{\Delta}\, P(s_2+j\,\frac{2\pi m}{\Delta}) \qquad (19)$$

where

$$Q(s_2) = \frac{P(s_2)}{1-e^{-(s_1+s_2+c)\Delta}} = \frac{1-e^{-(s_2+c-a)\Delta}}{(s_2+b)(s_2+c-a)(1-e^{-(s_1+s_2+c)\Delta})} \qquad (20)$$

Then,

$$G(z_1,z_2) = \frac{z_1^{-1}\, e^{-a\Delta}\, (1-e^{-(c-a)\Delta}\, z_2^{-1})}{(c-a-b)(1-e^{-a\Delta}\, z_1^{-1})(1-e^{-c\Delta} z_1^{-1} z_2^{-1})} \frac{(e^{-b\Delta} - e^{-(c-a)\Delta})\, z_2^{-1}}{(1-e^{-(c-a)\Delta}\, z_2^{-1})(1-e^{-b\Delta}\, z_2^{-1})}$$

$$= \frac{z_1^{-1}\, z_2^{-1}\, (pq - r)}{(c-b-a)(1-p\, z_1^{-1})(1-q\, z_2^{-1})(1-r\, z_1^{-1}\, z_2^{-1})} \qquad (21)$$

with $p = e^{-a\Delta}$, $q = e^{-b\Delta}$, and $r = e^{-c\Delta}$

Note in the above we evaluate line integrals by contour integration, closing for convenience, in the left half plane in the first integral and in the right half plane in the second. Also note $\mathrm{Re}[s_1] > 0$, $\mathrm{Re}[s_2] > 0$ since $h_2(\tau_1,\tau_2)$ is causal.

Example 3

For $a = 1.025866$, $b = 3.250379$, $c = 5.753641$ and $\Delta = 0.05$ s, we have

$$\frac{1}{(s_1+a)(s_2+b)(s_1+s_2+c)} \leftrightarrow \frac{0.0575 z_1^{-1} z_2^{-1}}{1.477397(1-0.95z_1^{-1})(1-0.85z_2^{-1})(1-0.75z_1^{-1} z_2^{-1})}$$

Because of its importance we give the conversion pair, derived above, explicitly:

$$\frac{1}{(s_1+a)(s_2+b)(s_1+s_2+c)} \leftrightarrow \frac{z_1^{-1} z_2^{-1} (pq-r)}{(c-a-b)(1-pz_1^{-1})(1-qz_2^{-1})(1-rz_1^{-1} z_2^{-1})} \qquad (23)$$

(note p, q and r are the z-plane maps of the poles $-a$, $-b$ and $-c$; e.g., $p = e^{-a\Delta}$.)

An alternative derivation (in the time domain) of the above conversion pair can also be given. A block diagram description of the input-output relationship (of the elementary quadratic system of Fig. 3) in the z-domain is given in Fig. 8.

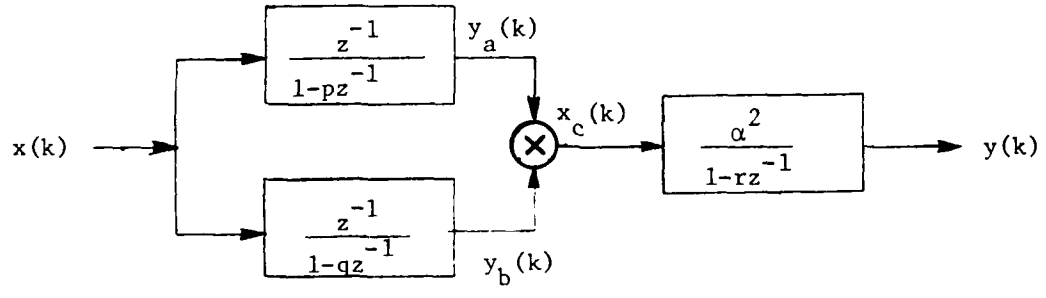

$$\alpha = (e^{-(a+b)\Delta} - e^{-c\Delta})/(c-a-b)$$

Fig. 8. Impulse-invariant z-domain characterization of the elementary quadratic system

Example 4

Let us calculate the response of the system of Example 2 for four sample points with k = 0, 1, 2, 3 and the input 1, 1, 0, 0, ... We find

$y_a(k)$: 0 1 1.95 1.8525

$y_b(k)$: 0 1 1.85 1.5725

so that their product gives the following input to the output block

$x_c(k)$: 0 1 3.6075 2.91306

Then y(k), as obtained from the difference equation $y(k) = 0.75y(k-1) + \alpha^2 x_c(k)$, $\alpha = 0.03892$, is

y(k): 0 0.00151 0.00660 0.00936

STEP-INVARIANT z-TRANSFORM FOR 1-M SECTION

The concept of step invariance of a two-dimensional linear system can be enunciated as follows. Given that a continuous input signal $\bar{x}(t_1, t_2)$ is applied to the sampled-data system of Fig. 9a; then the system of Fig. 9b is said to be step-invariant if its response $y(k_1, k_2)$ to the sequence $\bar{x}(k_1, k_2) = \bar{x}(k_1\Delta, k_2\Delta)$ equals the sampled response $\bar{y}(k_1\Delta, k_2\Delta)$ of Fig. 9a.

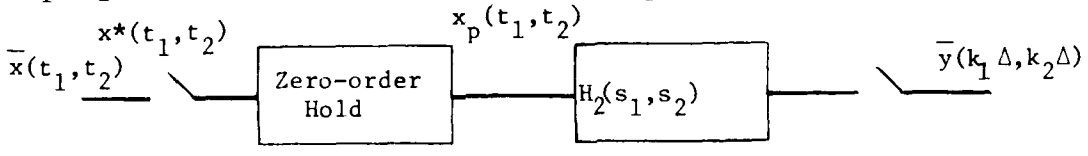

$$x_p(t_1, t_2) = \sum_{k_1,k_2=-\infty}^{\infty} \sum \bar{x}(k_1\Delta, k_2\Delta)\, p(t_1 - k_1\Delta)\, p(t_2 - k_2\Delta)$$

$p(t) = 1$ for $0 \leq t \leq \Delta$, 0 otherwise

(a) sampled-data system

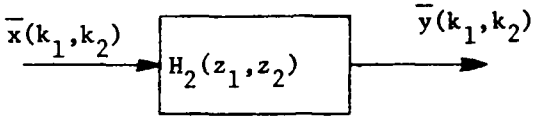

(b) Digital system

Fig. 9. Step-invariant digital system

The above concept immediately results in the following definition.

Definition. Given a continuous two-dimensional system H_a, a digital two-dimensional system H_d is said to be step invariant if the response of H_d to $u(k_1)\ u(k_2)$ equals the response of H_a to $u(t_1)\ u(t_2)$ at the sampled points.

Note that the above concept of step-invariance is a direct extension of this concept for the one dimensional case [13].

We begin the derivation by observing that the transfer function of the zero order hold is

$$H_{hold}(s_1, s_2) = \frac{(1 - e^{-s_1\Delta})(1 - e^{-s_2\Delta})}{s_1 s_2} \tag{24}$$

and the transfer function of the system between the ideal samplers (in Fig. 9a) is

$$\tilde{H}_2(s_1, s_2) = \frac{(1 - e^{-s_1\Delta})(1 - e^{-s_2\Delta})}{s_1 s_2} H_2(s_1, s_2)$$

$$= \frac{(1 - e^{-s_1\Delta} - e^{-s_2\Delta} + e^{-(s_1 + s_2)\Delta})}{s_1 s_2} H_2(s_1, s_2)$$

$$= \frac{1}{s_1 s_2} H_2(s_1, s_2) + \tag{25.1}$$

$$+ \frac{e^{-s_1\Delta}}{s_1 s_2} \quad H_2(s_1, s_2) \tag{25.2}$$

$$+ \frac{e^{-s_2\Delta}}{s_1 s_2} \quad H_2(s_1, s_2) \tag{25.3}$$

$$+ \frac{e^{-(s_1 + s_2)\Delta}}{s_1 s_2} \quad H_2(s_1, s_2) \tag{25.4}$$

Further, we make the important observation that the step-invariance of $H_2(s_1, s_2)$ to some $H_2(z_1, z_2)$ is equivalent to the impulse invariance of $\tilde{H}_2(s_1, s_2)$ to the same $H_2(z_1, z_2)$. This is obvious from the enunciation of the basic concepts of impulse and step invariance.

We will now restrict our attention to the 1M section so that

$$H_2(s_1, s_2) = \frac{ABC}{(s_1 + a)(s_2 + b)(s_1 + s_2 + c)} \tag{26}$$

Observe that each of the four terms on the right hand side of (25) is of the form

$$H_{2,i}(s_1, s_2) = \frac{e^{-(\mu s_1 + \nu s_2)}}{s_1 s_2} \frac{ABC}{(s_1 + a)(s_2 + b)(s_1 + s_2 + c)}$$

$$\mu, \nu = 0 \text{ or } \Delta$$

$$i = 1, 2, 3, 4 \tag{27}$$

Partial fraction expansion yields

$$H_{2,i}(s_1, s_2) = \frac{ABC}{ab} e^{-(\mu s_1 + \nu s_2)} \left[\frac{1}{s_1} - \frac{1}{s_1 + a}\right]\left[\frac{1}{s_2} - \frac{1}{s_2 + b}\right] \frac{1}{(s_1 + s_2 + c)}$$

$$= \frac{ABC}{ab} e^{-(\mu s_1 + \nu s_2)} \left[\frac{1}{s_1 s_2} - \frac{1}{s_1(s_2 + b)} - \frac{1}{s_2(s_1 + a)} + \frac{1}{(s_1 + a)(s_2 + b)}\right] \cdot$$

$$\frac{1}{s_1 + s_2 + c} \tag{28}$$

In turn, each of the four terms on the right hand side of (29) is of the form

$$G(s_1,s_2) = K\, e^{-(\mu s_1 + \nu s_2)} \frac{1}{(s_1+\alpha)(s_2+\beta)(s_1+s_2+\gamma)} \tag{29}$$

for which the impulse-invariant z-transform (from (23)) is

$$G(z_1,z_2) = K\, z_1^{-\mu}\, z_2^{-\nu} \frac{z_1^{-1}\, z_2^{-1}(\pi\xi-\rho)}{(\gamma-\alpha-\beta)(1-\pi z_1^{-1})(1-\xi z_2^{-1})(1-\rho z_1^{-1} z_2^{-1})} \tag{30}$$

Using the property of linearity, the step-invariant z-transform of $H_2(s_1,s_2)$ consists of sixteen terms obtained by using the partial fraction expansion of (28) in (25) and finally using the correspondence of (29)-(30) upon each term. The result is

$$H_2(z_1,z_2) = \frac{ABC}{ab} \frac{z_1^{-1}\, z_2^{-1}}{1 - r\, z_1^{-1} z_2^{-1}} \left\{ \frac{1-r}{c} + \frac{p-r}{c-a} \frac{1 - z_1^{-1}}{1 - p\, z_1^{-1}} + \frac{q-r}{c-b} \frac{1 - z_2^{-1}}{1 - q\, z_2^{-1}} + \frac{pq-r}{c-a-b} \frac{(1-z_1^{-1})(1-z_2^{-1})}{(1-pz_1^{-1})(1-q\, z_2^{-1})} \right\}$$

where $p = e^{-a\Delta}$, $q = e^{-b\Delta}$, $r = e^{-c\Delta}$.

This is represented in block-diagram form in Fig. 10.

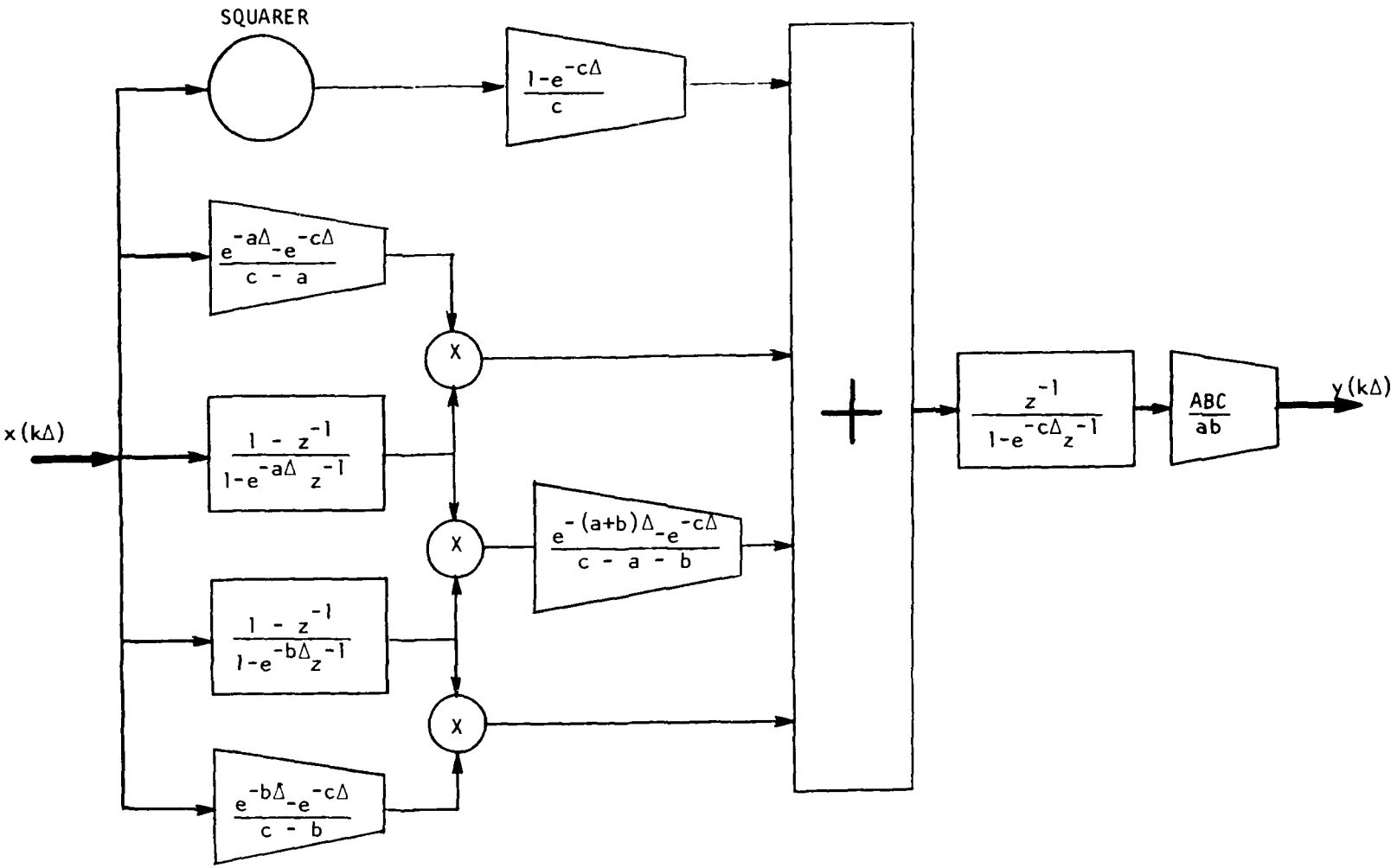

Fig. 10. Block diagram of step-invariant z-transform for the 1 - M section

III. DFT BASED COMPUTATION OF QUADRATIC VOLTERRA RESPONSE

A general method for computation of the response of a second order Volterra system (see Fig. 11) is highly useful in the investigation of Volterra system identification. The features desired in such a method are the following:

a. The characterization of the blocks in Fig. 11 should be permitted in

   s domain

   z domain

   f domain (i.e., in terms of the frequency ch. H(f(k)))

   t domain (i.e., in terms of the impulse response h(t(k)))

b. The specification of the input should be permissible in the time domain. This is useful in transient type of tests, such as with pulse inputs.

c. The specification of the input should be permissible in the frequency domain. This is useful in steady-state sinusoidal tests.

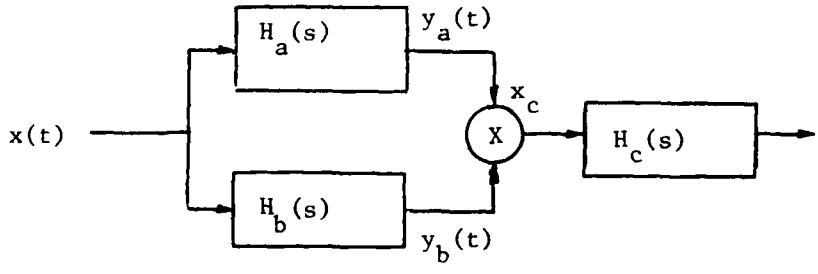

Fig. 11. Quadratic Volterra system

Such a method can be best developed by use of the discrete Fourier transform (DFT). We shall in fact use the fast, algorithmic version commonly known as the fast Fourier transform (FFT). And, we will use the terms DFT and FFT interchangably. To develop the method we begin first with the case of the linear system.

3.1 Linear System Response via DFT

Consider a linear system described by a z-domain transfer function H(z). Note that if an s-domain transfer function is given instead, then its z-domain pulse-equivalent function can be obtained by use of the FORTRAN program STOZ[10]. An example is the following

$$\frac{(10^4)s}{s^2 + 4(10^3)s + 10^8} \quad \leftrightarrow \quad \frac{0.02z^{-1} - 0.0196117z^{-2}}{1 - 1.884802z^{-1} + 0.923116z^{-2}}$$

where a sampling of $\Delta = 0.02$ ms. has been used.

The choice of the sampling interval and the number of points to be used in simulation generally requires some experimentation. However, certain guidelines may be given based upon signal theoretic considerations. These will be discussed later, and we assume that the sampling interval Δ, an input (of essential length b second, or B samples) x(t), and the number of points N to be used for DFT processing have been selected.

Notation -

Δ = Sampling interval

N = Number of samples used in DFT

$L = \frac{N}{2} + 1$

$T = N\Delta$

$\delta = \frac{1}{T}$, i.e., spacing of DFT frequencies,

or frequency resolution in DFT

$H(s)$ = s-domain transfer function

$H(z)$ = z-domain transfer function

$H(f_m)$ = Frequency characteristic of the network,

where $f_m = m$

$H(t_k)$ = Impulse response of the network, where $t_k = k\Delta$

$f_{max} = L\delta = (\frac{N}{2} + 1)\delta$, i.e., the highest unambiguous frequency

Whatever the specification of the linear system, we convert it to the $H(f_m)$ form as shown in the flowchart of Fig. 12.

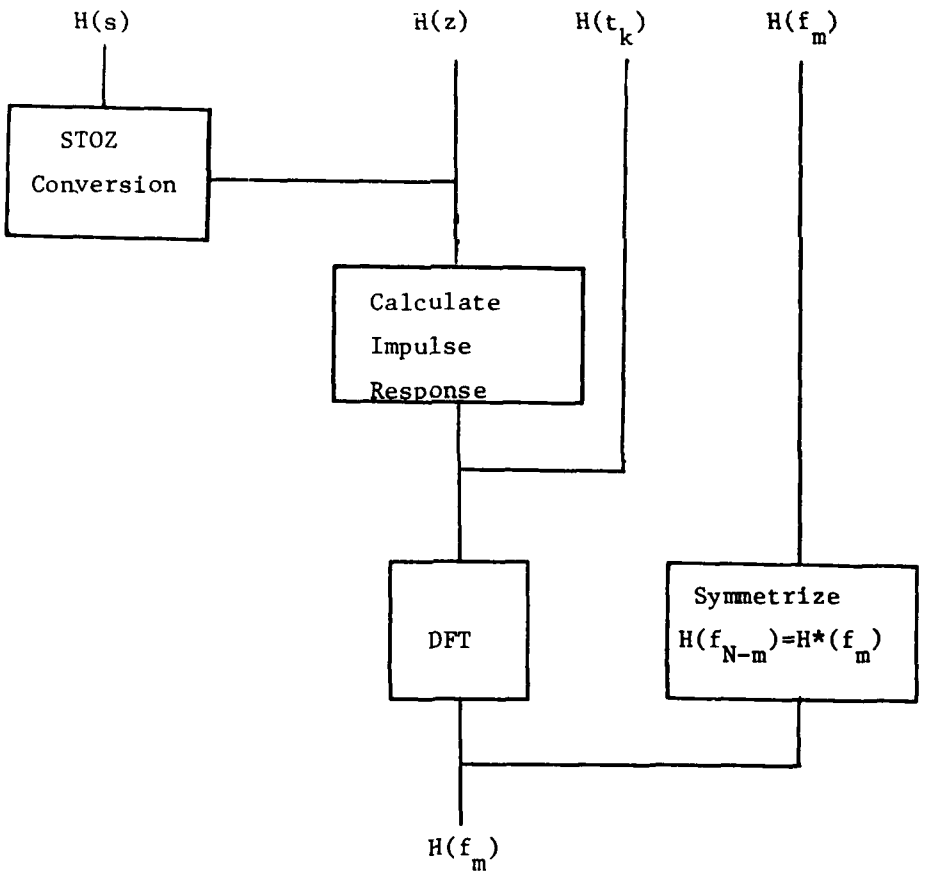

Fig. 12. Conversion of system specification to conjugate symmetric $H(f_m)$ form

Also, the input is converted to the frequency form as shown in Fig. 13.

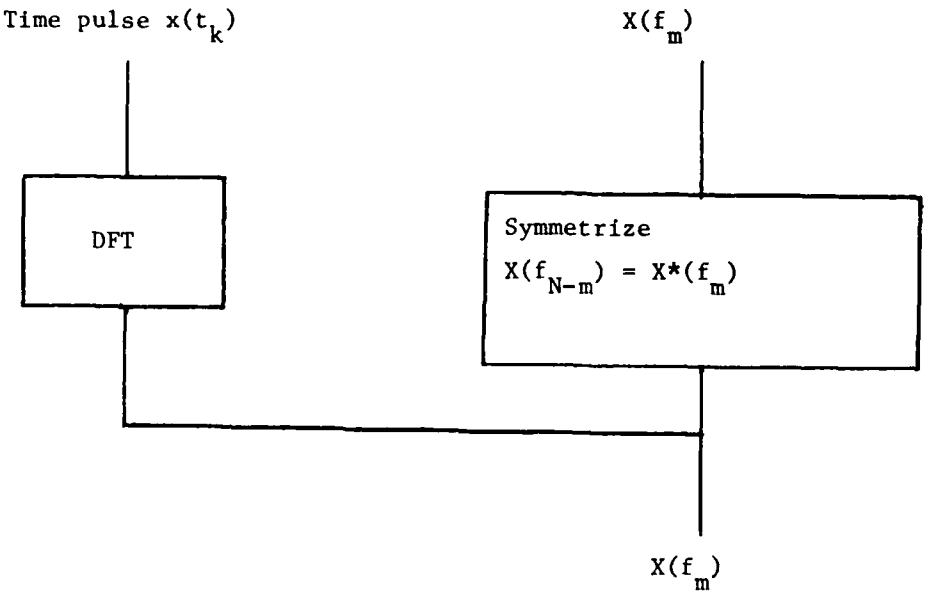

Fig. 13. Conversion of input to conjugate symmetric $X(f_m)$ form.

For purposes of quick reference we give below the pair of discrete Fourier transform formulas:

$$X(f_m) = \sum_{k=0}^{N-1} x(t_k) \; e^{-j \frac{2\pi}{N} mk} \tag{32a}$$

$$x(t_k) = \frac{1}{N} \sum_{m=0}^{N-1} X(f_m) \; e^{j \frac{2\pi}{N} mk} \tag{32b}$$

These relationships will also be written for convenience as

$$x(t_k) \underset{\text{DFT}^{-1}}{\overset{\text{DFT}}{\rightleftarrows}} X(f_m)$$

Then the network response can be obtained as

$$Y(f_m) = H(f_m)\, X(f_m) \tag{33a}$$

$$y(t_k) = DFT^{-1}\, Y(f_m) \tag{33b}$$

We remark for completeness that $y(t_k)$, the result of (33b) is equivalent to the following circular convolution [3]

$$y(t_k) = \sum_{j=0}^{N-1} x(t_j)\, h((t_k - t_j)) \tag{34}$$

where $((t_k - t_j))$ denotes the difference of t_k and t_j on a circular (or periodic) basis on a circle of circumference $T = N\Delta$. Formula (34) brings into focus two important facts. Formula (34), or equivalently (33b), can approximate the familiar aperiodic convolution integral

$$y(t) = \int_{-\infty}^{\infty} x(\tau)\, h(t-\tau)\, d\tau \tag{35}$$

if

a. it is multiplied by Δ, and

b. $A + B - 1 \leq N$, or $a + b \leq T$ (36)

where

a = duration of impulse response in seconds

A = duration of impulse response in samples

b = duration of input pulse in seconds

B = duration of input pulse in samples

Example 5

The simple first order system considered is

$$\frac{1}{s + 0.5} \quad \leftrightarrow \quad \frac{0.09754z^{-1}}{1 - 0.95123z^{-1}}$$

which has a cutoff frequency at approximately 0.08 Hz. Since the roll-off rate is -20dB/decade, it is reasonable to take the highest frequency of interest as f_{max} = 5 Hz. Thus we take the sampling interval to be Δ = 0.1s. Now since the time constant of the network is 2 sec, we should estimate the impulse response to be about 8s. Allowing for an input duration of 1s, we could take T to be 10s. However, for reasons of frequency resolution (discussed later) we use

$$N = 256$$

$$T = N\Delta = 25.6s$$

Two test inputs are examined below.

(a) Square pulse input - width b = 1 sec (B = 10 samples)

The true response is easily found to be

$$y(t) = 2[1 - e^{-0.5t}]\, u(t) - 2\,[1 - e^{-0.5(t-1)}]\, u(t - 1)$$

where u(t) denotes the unit step function. The samples $y(t_k)$ computed by the DFT method (via program VOL 2 - Section IV) are compared with the true value in Table 1; a graphical comparison is given in Fig. 14.

Table 1

t_k	0	0.1	0.2	0.5	1.0	2.0	5.0
True $y(t_k)$	0.0	0.0975	0.190	0.442	0.787	0.477	0.107
DFT based $y(t_k)$	0.0	0.0975	0.190	0.442	0.787	0.477	0.106

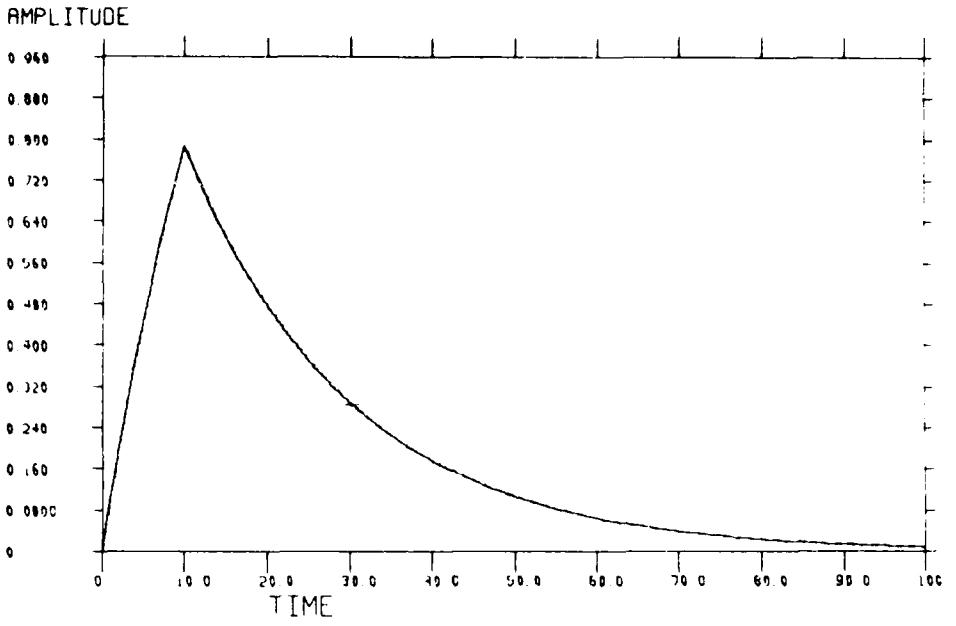

Fig. 14. Comparison of true and DFT-based responses (Example 5 - Square pulse input)

Exponential Input - $x(t) = e^{-0.25t}$

Because of the long duration of the input the number of points was increased to N = 512.

The true response is readily checked to be

$$y(t) = 4(e^{-0.25t} - e^{-0.5t})\ u(t)$$

The samples $y(t_k)$ computed by the DFT method (via program VOL2) are compared with the true values in Table 2; a graphical comparison is given in Fig. 15.

Table 2

t_k	0.0	0.1	0.2	0.5	1.0	2.0	5.0	10.0
True $y(t_k)$	0.0	0.0963	0.186	0.415	0.689	0.955	0.818	0.301
DFT based $y(t_k)$	0.0	0.0975	0.188	0.420	0.698	0.967	0.828	0.305

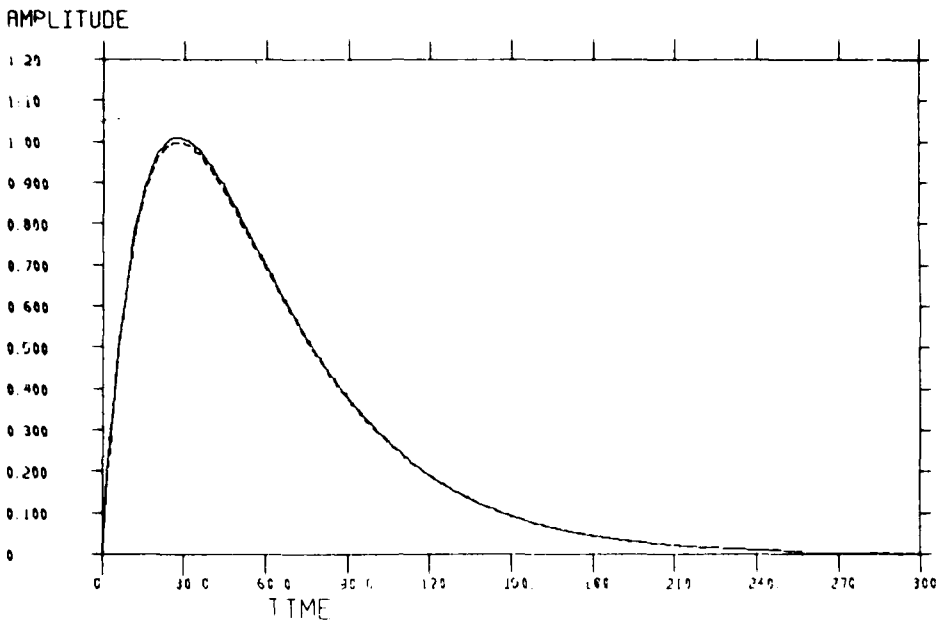

Fig. 15. Comparison of true and DFT-based responses (Example 5 - Exponential input)

It is seen above that the DFT method is able to compute the network response quite accurately. For further accuracy, the sampling interval must be decreased or the number of points must be increased or both. We should also remark that if the input were e^{-t}, a sampling interval of 0.05s. would be used rather than 0.1s.

Example 6

The oscillatory system considered is

$$\frac{(10^4)s}{s^2 + 4(10^3)s + 10^8} \quad \leftrightarrow \quad \frac{0.02z^{-1} - 0.0196117z^{-2}}{1 - 1.884802z^{-1} + 0.923116z^{-2}}$$

which has a natural frequency at approximately 1.6 KHz. Since the roll-off rate is -40dB/decade it is reasonable to take the highest frequency of interest as f_{max} = 25 KHz. Thus we take the sampling interval to be Δ = 0.02 ms.

Further, since the time constant is 0.5 ms, we should estimate the duration of the impulse response to be about 2 ms. Allowing for an input signal duration of 0.5 ms, we could take T to be 2.5 ms. However, for reasons of frequency resolution (discussed later) we use

$$N = 512$$

$$T = N\Delta = 10.24 \text{ ms}$$

The test input is taken to be a square pulse of width b = 0.6 ms. (B = 30 samples). Correspondingly, the true response is

$$y(t) = e^{-2(10^3)t} \sin(10^4 t)\, u(t) - e^{-2(10^3)(t-b)} \sin(10^4(t-b))\, u(t-b).$$

The samples $y(t_k)$ computed by the DFT method (via program VOL2) are compared with the tru values in Table 3; a graphical comparison is given in Fig. 16.

Table 3

t_k ms	0	0.02	0.04	0.1	0.2	0.5	1.0
True $y(t_k)$	0.0	0.191	0.359	0.689	0.610	-0.353	0.266
DFT based $y(t_k)$	0.0	0.191	0.360	0.694	0.633	-0.369	0.271

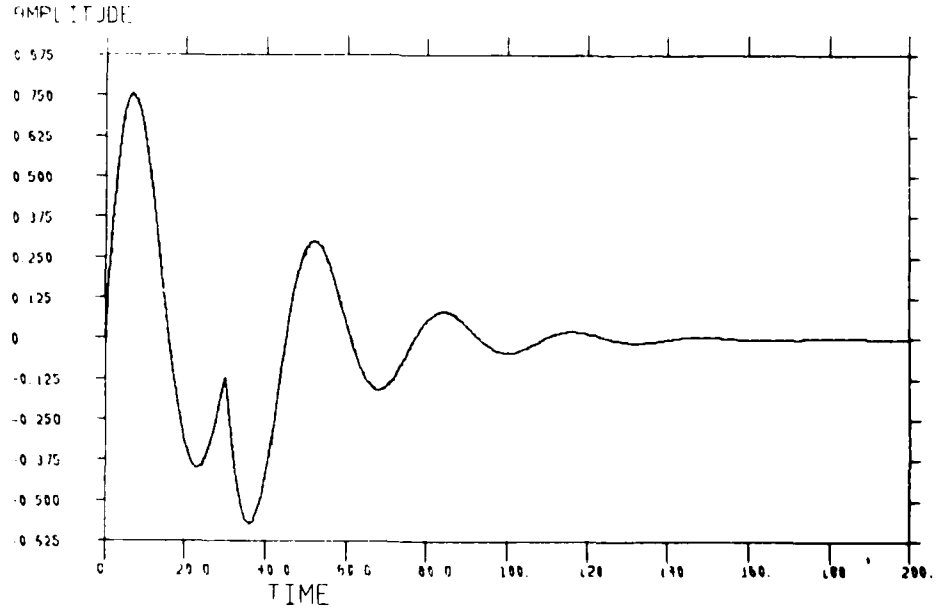

Fig. 16. Comparison of true and DFT-based responses (Example 6)

Again, as in Example 1, a close correspondence between the true and DFT based responses is evidenced.

Example 7

Here we consider the case where the network specification is given in terms of its impulse response

$$h(t) = 1 \quad \text{for} \quad 0 \leq t \leq 10 \text{ ms.}$$

$$0 \quad \text{otherwise}$$

The input is specified as a square pulse of duration 20 ms, i.e.,

$$x(t) = 1 \quad \text{for} \quad 0 \leq t \leq 20 \text{ ms}$$

$$0 \quad \text{otherwise}$$

We will use $\Delta = 1$ ms and $N = 128$. The response computed from the DFT based program is compared with the true response in Fig. 17. As expected, good agreement has been realized.

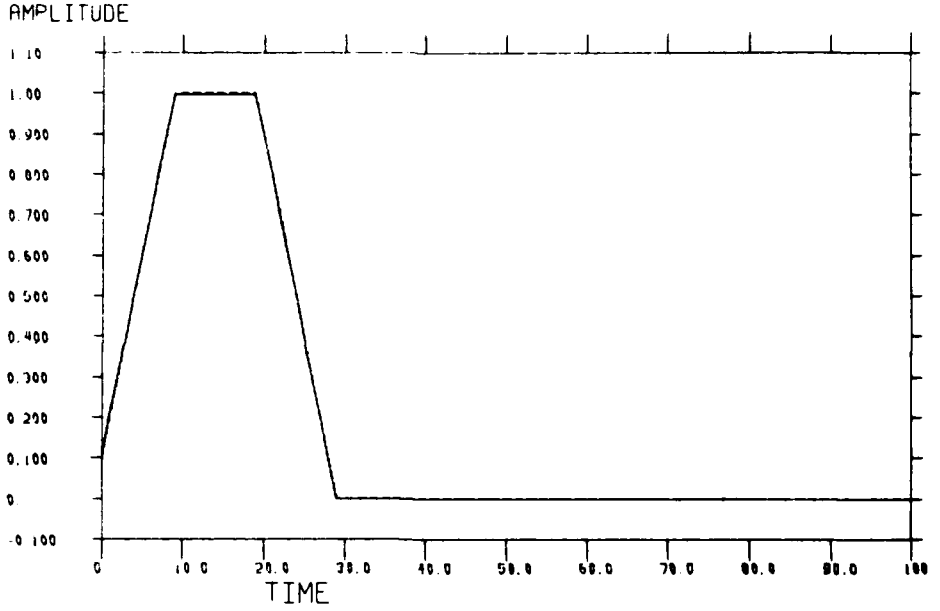

Fig. 17. Comparison of true and DFT-based responses (Example 7)

Example 8

In this final example the network specification is given in terms of the frequency response

$$H(f) = 1 \quad \text{for} \quad |f| \leq 5 \text{ KHz}$$

and a square pulse input

$$x(t) = 1 \text{ for } 0 \leq t \leq 0.2 \text{ ms}$$

Since the input is a square pulse of width 0.2 ms the highest frequency of interest f_{max} is estimated at 10 f_{zero} = 50 KHz. Thus the sampling frequency must be 100 KHz requiring $\Delta = 10\,\mu s$. Then we have

Input duration = 0.2 ms (20 samples)

Impulse response

$$\text{duration} \cong 20\ t_{zero} = 2 \text{ ms}$$

$$\equiv 200 \text{ samples}$$

We therefore take N = 512. The true response is known to be

$$y(t) = \frac{1}{\pi} \{Si[10\pi(10^3)t] - Si[10\pi(10^3)(t - 0.2(10^{-3}))]\}$$

where

$$Si[V] = \int_0^V \frac{Sin(v)}{v}\, dv$$

The samples $y(t_k)$ computed by the DFT method are compared with the true value in Table 3. A graphical sketch of the computed values is given in Fig. 18. (Note that the true response is not shown in Fig. 18).

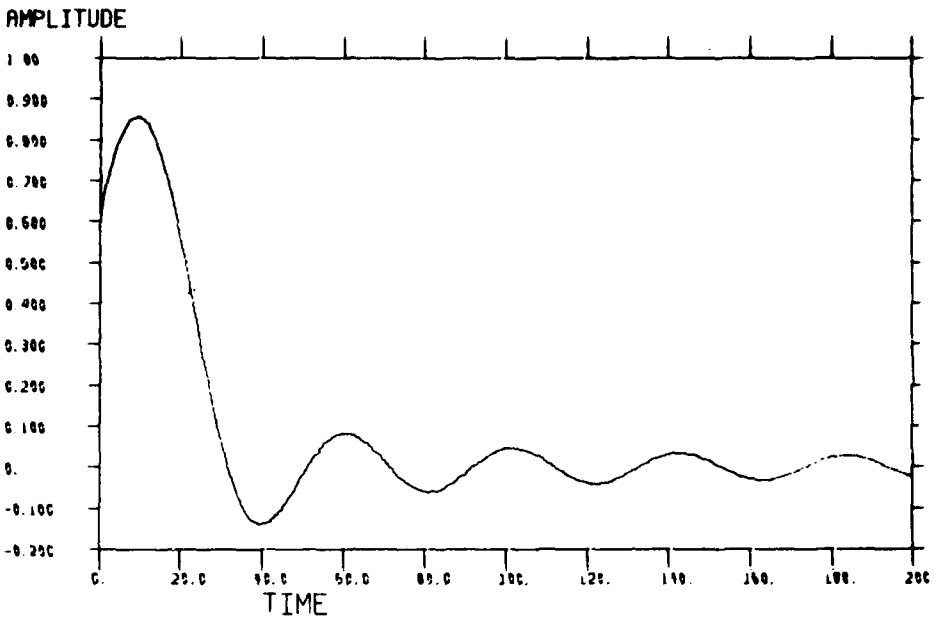

Fig. 18. DFT-based response - Example 9

IV. BILINEAR AND VOLTERRA RESPONSES OF 1-M SECTION TO SQUARE PULSE INPUTS

Our interest in the response of nonlinear Volterra systems to square-pulses arises because of the many advantages this type of input offers in the laboratory. These are: (a) it is easily generated in the laboratory, (b) its spectral width (f_b) is readily specifiable through the pulse width ($b = 1/f_b$), and (c) the formulas for the system response are tractable. Also, as we shall see in the next section, it is possible to perform parameter identification via pencil-of-function method for such input-output pairs.

In addition to the Volterra response of the 1-M section (see Fig. 19), we will also be interested in its bilinear response, because the bilinear response $V_2\{x_1,x_2\}$ can be determined in the laboratory by performing tests upon the system with the inputs $x_1 + x_2$ and $x_1 - x_2$ and then using the formula [2]

$$V_2\{x_1,x_2\} = \frac{1}{4}\left[V_2[x_1 + x_2] - V_2[x_1 - x_2]\right] \tag{37a}$$

Alternatively, one can test the system with the inputs x_1, x_2 and $x_1 + x_2$. Then the bilinear response is given by

$$V_2\{x_1,x_2\} = \frac{1}{2}\left[V_2[x_1 + x_2] - V_2[x_1] - V_2[x_2]\right] \tag{37b}$$

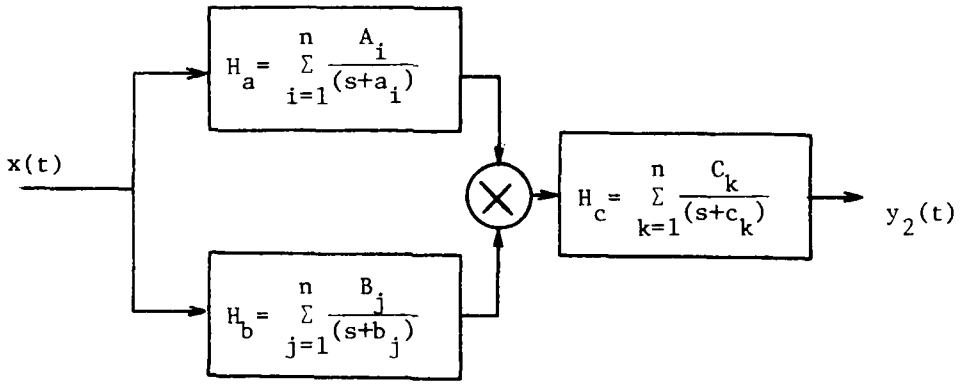

Fig. 19 General 1-M Section

[2] Formulas (37a) and (37b) assume that the Kernel $H_2(s_1,s_2)$ is symmetric.

Of course, the real reason for the interest in the bilinear response is its bilinearity property. For example, the bilinear response to two square pulses $p_1(t) = A(u(t)-u(t-T_1)) = A(u_o-u_1)$ and $p_2(t) = B(u(t-T_1)-u(t-T))=B(u_1-u_2)$ is given as

$$V_2\{p_1,p_2\} = AB[V_2\{u_o,u_1\} - V_2\{u_1,u_1\} - V_2\{u_o,u_2\} + V_2\{u_1,u_2\}] \qquad (38)$$

4.1 Bilinear Response to Step Inputs

4.1.1 Elementary 1-M Section

Consider that $x_1(t) = u(t - \alpha)$ and $x_2(t) = u(t - \beta)$ with $\beta > \alpha$. Then the associated bilinear response of the elementary 1-M section (see Fig. 3) is given by

$$\begin{aligned}\overline{Y}_2(s_1,s_2) &= H_2(s_1,s_2)\, X_1(s_1)\, X_2(s_2)\\ &= \frac{1}{(s_1+a)(s_2+b)(s_1+s_2+c)} \quad \frac{e^{-\alpha s_1}}{s_1} \quad \frac{e^{-\beta s_2}}{s_2}\\ &= \frac{1}{ab}\left(\frac{1}{s_1} - \frac{1}{s_1+a}\right)\left(\frac{1}{s_2} - \frac{1}{s_2+b}\right) \quad \frac{e^{-\alpha s_1}\, e^{-\beta s_2}}{s_1 + s_2 + c}\end{aligned}$$

so that, by application of George's theorem [8], the bilinear response becomes

$$V_2\{X_1(s),X_2(s)\} = \frac{e^{-\beta s}}{ab}\left[\frac{1}{s(s+c)} - \frac{1}{(s+b)(s+c)} - e^{-a(\beta-\alpha)}\left(\frac{1}{(s+a)(s+c)} - \frac{1}{(s+a+b)(s+c)}\right)\right]$$

$$= \frac{e^{-\beta s}}{ab}\left[\frac{1}{cs} - \frac{e^{-a(\beta-\alpha)}}{(c-a)} \quad \frac{1}{s+a} - \frac{1}{(c-b)} \quad \frac{1}{s+b}\right.$$

$$+ \frac{e^{-a(\beta-\alpha)}}{(c-a-b)} \quad \frac{1}{s+a+b}$$

$$\left.\left(-\frac{1}{c} + \frac{1}{c-b} + e^{-a(\beta-\alpha)}\left(\frac{1}{c-a} - \frac{1}{c-a-b}\right)\right) \frac{1}{s+c}\right]$$

$$= \frac{e^{-\beta s}}{ab}\left[\frac{1}{cs} - \frac{e^{-a(\beta-\alpha)}}{(c-a)} \quad \frac{1}{s+a} - \frac{1}{(c-b)(s+b)} + \frac{e^{-a(\beta-\alpha)}}{(c-a-b)} \quad \frac{1}{s+a+b}\right.$$

$$\left. + \left(\frac{b}{c(c-b)} - \frac{be^{-a(\beta-\alpha)}}{(c-a)(c-a-b)}\right) \frac{1}{s+c}\right] \qquad (39)$$

Therefore the bilinear response in time domain is

$$V_2\{x_1,x_2\} = \frac{1}{ab}[d_o - d_1 L e^{-at'} - d_2 e^{-bt'} + d_3 L e^{-(a+b)t'} + (d_4 - d_5 L) e^{-ct'}]u(t') \quad (40a)$$

where $L = e^{-a(\beta-\alpha)}$, $t' = t - \beta$ and

$$d_0 = 1/c \quad (40b)$$

$$d_1 = 1/(c-a) \quad (40c)$$

$$d_2 = 1/(c-b) \quad (40d)$$

$$d_3 = 1/(c-a-b) \quad (40e)$$

$$d_4 = b/c(c-b) \quad (40f)$$

$$d_5 = b/(c-a)(c-a-b) \quad (40g)$$

Similarly, for the case $\alpha > \beta$, we obtain

$$V\{x_1,x_2\} = \frac{1}{ab}[d_o - d_1 e^{-at'} - d_2 M e^{-bt'} + d_3 M e^{-(a+b)t'} + (d_6 - M d_7) e^{-ct'}]u(t') \quad (40h)$$

where $M = e^{-b(\alpha-\beta)}$, $t' = t-\alpha$ and

$$d_6 = a/c(c-a) \quad (40i)$$

$$d_7 = a/(c-b)(c-a-b) \quad (40j)$$

Note that $d_4 - d_5 = d_6 - d_7$.

4.1.2 General 1-M Section

For the general 1-M section of Fig. 19, the bilinear response to the unit steps $x_1(t) = u(t-\alpha)$ and $x_2(t) = u(t-\beta)$ is obtained immediately from formula (17) and (40a). That is,

$$V\{x_1,x_2\} =$$

$$\sum_{i,j,k=1}^{n} \frac{1}{a_i b_j}[d_o^{ijk} - d_1^{ijk} L^{ijk} e^{-a_i t'} - d_2^{ijk} e^{-b_j t'} + d_3^{ijk} L^{ijk} e^{-(a_i+b_j)t'} + (d_4^{ijk} - d_5^{ijk} L^{ijk}) e^{-c_k t'}] u(t') \quad (41)$$

where the constants are defined as in (40) with a_i, b_j and c_k substituted in place of a, b, and c. For example,

$$d_1^{ijk} = \frac{1}{c_k - a_i}$$

and

$$L^{ijk} = e^{-a_i(\beta-\alpha)}$$

4.1.3 Symmetric 1-M Section

Since the bilinear response can be measured only for the symmetric Kernel it is useful to give the counterparts of (40a) and (41) for this case. For the elementary 1-M section, setting b = a we have

$$V\{x_1,x_2\} = \frac{1}{a^2}\left[d_o-(d_1L+d_2)e^{-at'}+d_3Le^{-2at'}+(d_4-d_5L)e^{-ct'}\right]u(t') \qquad (42)$$

Similarly, for the general 1-M section, setting $b_j = a_j$, we have

$$V\{x_1,x_2\} =$$

$$\sum_{i,j,k=1}^{n} \frac{1}{a_i a_j}\left[d_o^{ijk} - d_1^{ijk} L^{ijk} e^{-a_i t'} - d_2^{ijk} e^{-a_j t'} + d_3^{ijk} L^{ijk} e^{-(a_i+a_j)t'} + (d_4^{ijk} - d_5^{ijk} L^{ijk}) e^{-c_k t'} \right] u(t') \qquad (43)$$

4.2 Bilinear Response to Square Pulses

4.2.1 Elementary 1-M Section

We are interested in finding the bilinear response of the 1-M section to the input pair $p_1(t) = u(t) - u(t-T_1)$, $p_2(t) = u(t-T_1) - u(t-T)$. The associated bilinear response (in s-domain) is

$$Y_{(2)}(s_1,s_2) = H_2(s_1,s_2)\, X(s_1)X(s_2)$$

$$= \frac{1}{(s_1+a)(s_2+b)(s_1+s_2+c)} \cdot \frac{(1-e^{-T_1 s_1})}{s_1} \cdot \frac{(e^{-T_1 s_2} - e^{-Ts_2})}{s_2}$$

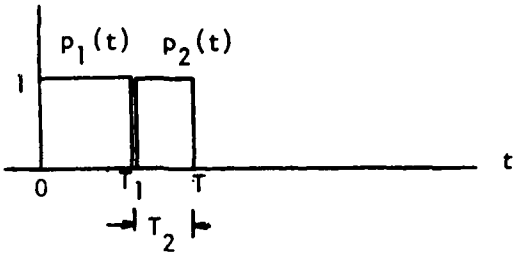

Fig. 20 Square pulse - Input pair

From this we can obtain the bilinear response by application of George's theorem. Alternatively, the desired bilinear response is computed using the bilinearity property:

$$V_2\{p_1,p_2\} = V_2\{u_o,u_1\} - V_2\{u_1,u_1\} - V_2\{u_o,u_2\} + V_2\{u_1,u_2\}$$

where $u_o = u(t)$, $u_1 = u(t-T_1)$ and $u_2 = u(t-T)$.

By use of formula (40), we obtain

$$V_2\{p_1,p_2\} =$$

$$\frac{1}{ab}\Big[[d_o-d_1L_1e^{-at'}- d_2e^{-bt'}+ d_3L_1e^{-(a+b)t'}+(d_4-d_5L_1)e^{-ct'}]\,u(t')$$

$$-[d_o-d_1e^{-at'}-d_2e^{-bt'}+d_3e^{-(a+b)t'}+(d_4-d_5)e^{-ct'}]u(t')$$

$$-[d_o-d_1L\,e^{-at''}- d_2e^{-bt''}+ d_3L\,e^{-(a+b)t''}+ (d_4-d_5L\,)e^{-ct''}]\,u(t'')$$

$$+[d_o-d_1L_2e^{-at''}- d_2e^{-bt''}+ d_3L_2e^{-(a+b)t''}+ (d_4-d_5L_2)e^{-ct''}]\,u(t'')\Big] \qquad (44a)$$

where

$$L_1 = e^{-aT_1} \qquad (44b)$$

$$L_2 = e^{-aT_2} = e^{-a(T-T_1)} \qquad (44c)$$

$$L = e^{-aT} \qquad (44d)$$

$$t' = t - T_1 \qquad (44e)$$

$$t'' = t - T \qquad (44f)$$

Let us also define, for convenience,

$$M_2 = e^{-bT_2} \tag{44g}$$

$$N_2 = e^{-cT_2} \tag{44h}$$

Then simplification of (44a) yields

$$V_2\{p_1,p_2\} =$$

$$\begin{cases} 0 & \text{for } 0 \le t < T_1 \\ \dfrac{(1-L_1)}{ab}[d_1 e^{-at'} - d_3 e^{-(a+b)t'} + d_5 e^{-ct'}]\, u(t') & \text{for } T_1 \le t < T \\ \dfrac{1-L_1}{ab}[d_3 L_2 (1-M_2)\, e^{-(a+b)t''} + d_5 (N_2 - L_2) e^{-ct''}] & \text{for } T \le t \end{cases} \tag{44i}$$

4.2.2 General 1-M Section

For the general 1-M section of Fig. 19, the bilinear response to the square pulses $p_1(t)$ and $p_2(t)$ is obtained immediately from formulas (17) and (44i). That is,

$$V_2\{p_1,p_2\} =$$

$$\begin{cases} 0 & \text{for } 0 \le t < T_1 \\ \displaystyle\sum_{i,j,k=1}^{n} A_i B_j C_k \frac{(1-L_1^{ijk})}{a_i b_j}[d_1^{ijk} e^{-a_i t'} - d_3^{ijk} e^{-(a_i+b_j)t'} + d_5^{ijk} e^{-c_k t'}]\, u(t') & \text{for } T_1 \le t < T \\ \displaystyle\sum_{i,j,k=1}^{n} A_i B_j C_k \frac{(1-L_1^{ijk})}{a_i b_j}[d_3^{ijk} L_2^{ijk} (1-M_2^{ijk}) e^{-(a_i+b_j)t''} + d_5 (N_2^{ijk} - L_2^{ijk}) e^{-c_k t''}]\, u(t'') & \text{for } T \le t \end{cases} \tag{45}$$

where the constants are defined as in (40) and (44) with a_i, b_j and c_k substituted in place of a,b,c. For example

$$d_1^{ijk} = 1/(c_k - a_i)$$

and

$$L_1^{ijk} = e^{-a_i T_1}$$

4.2.3 Symmetric 1-M Case

Since the bilinear response can be measured only for the symmetric Kernel, it is useful to give the counterparts of (44i) and (45) for this case. For the elementary 1-M section, setting b = a we have

$$V_2\{p_1,p_2\} =$$

$$\begin{cases} 0 & \text{for } 0 \le t < T_1 \\ \dfrac{1-L_1}{a^2}\left[\, d_1 e^{-at'} - d_3 e^{-2at'} + d_5 e^{-ct'}\right] u(t') & \text{for } T_1 \le t < T \\ \dfrac{1-L_1}{a^2}\left[\, d_3 L_2(1-L_2)e^{-2at'} + (N_2-L_2)d^{-ct''}\right] u(t'') & \text{for } T \le t \end{cases} \tag{46}$$

Similarly for the general 1-M section, setting $b_j = a_j$, we have

$$V_2\{p_1,p_2\} =$$

$$\begin{cases} 0 & \text{for } 0 \le t < T_1 \\ \sum_{i,j,k=1}^{n} A_i B_j C_k \dfrac{1-L_1^{ijk}}{a_i a_j}\left[\, d_1^{ijk} e^{-a_i t'} - d_3^{ijk} e^{-(a_i+a_j)t'} + d_5^{ijk} e^{-c_k t'}\right] u(t') & \text{for } T_1 \le t < T \\ \sum_{i,j,k=1}^{n} A_i B_j C_k \dfrac{(1-L_1^{ijk})}{a_i a_j}\left[\, d_3^{ijk} L_2^{ijk}(1-M_2^{ijk}) e^{-(a_i+a_j)t''} + (N_2^{ijk}-L_2^{ijk}) e^{-c_k t''}\right] u(t'') & \text{for } T \le t \end{cases} \tag{47}$$

Example 9

Consider an elementary 1-M section with

$$H_a(s) = H_b(s) = \frac{1}{s+1} - \frac{10}{s+5}$$

$$H_c(s) = 4/(s+12)$$

and $p_1(t) = u(t) - u(t-1)$, $p_2(t) = u(t-1) - u(t-2)$

Then using (4) we have

$V\{p_1,p_2\} =$

$$0 \qquad \text{for } 0 \le t < T$$

$$\left\{ \frac{A_1B_1C_1(1-L_1^{111})}{a_1b_1} \left[d_1^{111} e^{-a_1t'} - d_3^{111} e^{-(a_1+b_1)t'} + d_5^{111} e^{-c_1t'} \right] \right.$$

$$+ \frac{A_1B_2C_1(1-L_1^{121})}{a_1b_2} \left[d_1^{121} e^{-a_1t'} - d_3^{121} e^{-(a_1+b_2)t'} + d_5^{121} e^{-c_1t'} \right]$$

$$+ \frac{A_2B_1C_1(1-L_1^{211})}{a_2b_1} \left[d_1^{211} e^{-a_2t'} - d_3^{211} e^{-(a_2+b_1)t'} + d_5^{211} e^{-c_1t'} \right]$$

$$\left. + \frac{A_2B_2C_1(1-L_1^{221})}{a_2b_2} \left[d_1^{221} e^{-a_2t'} - d_3^{221} e^{-(a_2+b_2)t'} + d_5^{221} e^{-c_1t'} \right] \right\} u(t')$$

$$\text{for } T_1 \le t < T$$

$$\left\{ \frac{A_1B_1C_1(1-L_1^{111})}{a_1b_1} \left[d_3^{111} L_2^{111} (1-M_2^{111}) e^{-(a_1+b_1)t''} + (N_2^{111}-L_2^{111}) e^{-c_1t''} \right] \right.$$

$$+ \frac{A_1B_2C_1(1-L_1^{121})}{a_1b_2} \left[d_3^{121} L_2^{121} (1-M_2^{121}) e^{-(a_1+b_2)t''} + (N_2^{121}-L_2^{121}) e^{-c_1t''} \right]$$

$$\left. + \frac{A_2B_1C_1(1-L_1^{211})}{a_2b_1} \left[d_3^{211} L_2^{211} (1-M_2^{211}) e^{-(a_2+b_1)t''} + (N_2^{211}-L_2^{211}) e^{-c_1t''} \right] \right.$$

$$+ \frac{A_2B_2C_1(1-L_1^{221})}{a_2b_2} \left[d_3^{221}L_2^{221}(1-M_2^{221})e^{-(a_2+b_2)t''} + (N_2^{221}-L_2^{221})e^{-c_1t''} \right] \Bigg\} u(t'')$$

for $T \leq t$

where

$a_1 = b_1 = 1$ $\quad c_1 = 12$ $\quad c_2 = 0$

$A_1 = B_1 = 1$ $\quad C_1 = 4$ $\quad C_2 = 0$

$T_1 = T_2 = 1$ $\quad T = 2$

Thus

$V\{p_1, p_2\} =$

0 for $0 \leq t < 1$

$$\Bigg\{ 4(1-e^{-1}) \left[\frac{1}{11} e^{-t'} - \frac{1}{10} e^{-2t'} + \frac{1}{110} e^{-12t'} \right]$$

$$+ \frac{-40(1-e^{-1})}{(5)} \left[\frac{1}{11} e^{-t'} - \frac{1}{6} e^{-6t'} + \frac{5}{66} e^{-12t'} \right]$$

$$+ \frac{-40(1-e^{-5})}{(5)} \left[\frac{1}{7} e^{-5t'} - \frac{1}{6} e^{-6t'} + \frac{1}{42} e^{-12t'} \right]$$

$$+ \frac{400(1-e^{-5})}{(25)} \left[\frac{1}{7} e^{-5t'} - \frac{1}{2} e^{-10t'} + \frac{5}{14} e^{-12t'} \right] \Bigg\} u(t')$$

for $1 \leq t < 2$

$$\Bigg\{ 4(1-e^{-1}) \left[\frac{1}{10} e^{-1}(1-e^{-1})e^{-2t''} + (e^{-12}-e^{-1})e^{-12t''} \right]$$

$$+ \frac{-40(1-e^{-1})}{(5)} \left[\frac{1}{6} e^{-1}(1-e^{-5})e^{-6t''} + (e^{-12}-e^{-1})e^{-12t''} \right]$$

$$+ \frac{-40(1-e^{-5})}{(5)} \left[\frac{1}{6} e^{-5}(1-e^{-1})e^{-6t''} + (e^{-12}-e^{-5})e^{-12t''} \right]$$

$$+ \frac{400(1-e^{-5})}{(25)} \left[\frac{1}{2} e^{-5}(1-e^{-5})e^{-10t''} + (e^{-12}-e^{-5})e^{-12t''} \right] \Bigg\} u(t'')$$

for $2 \leq t$

$$
=
$$

$$
0 \qquad \text{for } 0 \leq t < 1
$$

$$
\Big\{ 0.229862e^{-(t-1)} - 0.252848e^{-2(t-1)} + 0.022986e^{-12(t-1)}
$$

$$
-0.459724e^{-(t-1)} + 0.842827e^{-6(t-1)} - 0.383103e^{-12(t-1)}
$$

$$
-1.135157e^{-5(t-1)} + 1.324349e^{-6(t-1)} - 0.189193e^{-12(t-1)}
$$

$$
2.270313e^{-5(t-1)} - 7.946096e^{-10(t-1)} + 5.6758\, e^{-12(t-1)} \Big\}\ u(t-1)
$$

$$
\text{for } 1 \leq t < 2
$$

$$
\Big\{ 0.058798e^{-2(t-2)} - 0.930161e^{-12(t-2)}
$$

$$
-0.307969e^{-6(t-2)} + 1.860322e^{-12(t-2)}
$$

$$
-0.005641e^{-6(t-2)} + 0.053492e^{-12(t-2)}
$$

$$
+0.053179e^{-10(t-2)} - 0.106983e^{-12(t-2)} \Big\}\ u(t-2)
$$

$$
\text{for } 2 \leq t
$$

$$
=
$$

$$
0 \qquad \text{for } 0 \leq t < 1
$$

$$
\Big\{ -0.229862e^{-(t-1)} + 1.135156e^{-5(t-1)} - 0.252848e^{-2(t-1)}
$$

$$
+\ 2.167176e^{-6(t-1)} - 7.946096e^{-10(t-1)} +\ 5.1265\, e^{-12(t-1)} \Big\}\ u(t-1)
$$

$$
\text{for } 1 \leq t < 2
$$

$$
\Big\{ 0.058798e^{-2(t-2)} - 0.31361e^{-6(t-2)}
$$

$$
+ 0.053179e^{-10(t-2)} + 0.87667e^{-12(t-2)} \Big\}\ u(t-2)
$$

$$
\text{for } 2 \leq t
$$

4.3 Volterra Response to Step Input

4.3.1 Elementary 1-M Section

The Volterra response to a unit step u(t) is obtained by setting $\alpha = \beta = 0$ and $L = 1$ in (40a):

$$y_2(t) = \frac{1}{ab}\,[d_o - d_1 e^{-at} - d_2 e^{-bt} + d_3 e^{-(a+b)t} + (d_4 - d_5)e^{-ct}]u(t) \tag{48}$$

where $d_o, \ldots, d_5$ are the same as in (40).

4.3.2 General 1-M Section

For the general 1-M section of Fig. 19 the Volterra response to a unit step u(t) is obtained by setting $\alpha = \beta = 0$ and $L^{ijk} = 1$ in (41):

$$y_2(t) = \sum_{i,j,k=1}^{n} \frac{1}{a_i b_j}\,[d_o^{ijk} - d_1^{ijk} e^{-a_i t} - d_2^{ijk} e^{-b_j t} + d_3^{ijk} e^{-(a_i+b_j)t} + (d_4^{ijk} - d_5^{ijk})\, e^{-c_k t}]\, u(t) \tag{49}$$

4.3.3 *Symmetric* 1-M Section

For the symmetric elementary 1-M section we have from (48)

$$y_2(t) = \frac{1}{a^2}[d_o - (d_1+d_2)e^{-at} + d_3 e^{-2at} + (d_4 - d_5)e^{-ct}]\, u(t) \tag{50}$$

Similarly, for the multiple pole case we have from (49)

$$y_2(t) = \sum_{i,j,k=1}^{n} \frac{1}{a_i a_j}\,[\, d_o^{ijk} - d_1^{ijk} e^{-a_i t} - d_2^{ijk} e^{-a_j t} + d_3^{ijk} e^{-(a_i+a_j)t} + (d_4^{ijk} - d_5^{ijk}) e^{-c_k t}\,]\, u(t) \tag{51}$$

4.4 Volterra Response to Square Pulse

4.4.1 Elementary 1-M Section

The Volterra response to a square pulse $p(t) = u(t) - u(t-\tau) \triangleq u_o - u_1$ is

$$y_2(t) = V_2\{u_o,u_o\} - V_2\{u_o,u_1\} - V_2\{u_1,u_o\} + V_2\{u_1,u_1\}$$

By use of (40a) and (40h), and some simplification, we have

$$y_2(t) =$$

$$\frac{1}{ab}\left[d_o - d_1\, d^{-at} - d_2\, e^{-bt} + d_3\, e^{-(a+b)t} + (d_4-d_5)\, e^{-ct'}\right] u(t')$$

$$0 \leq t < T$$

$$\frac{1}{ab}\left[d_3(L-1)(M-1)\, e^{-(a+b)t} + ((d_4-d_5)N+d_5L+d_7M-d_5-d_6)e^{-ct}\right] u(t)$$

$$T < t \qquad (52)$$

where $t' = t-T$, $L = e^{-aT}$, $M = e^{-bT}$ and $N = e^{-cT}$. All other symbols are the same as in (40).

4.4.2 General 1-M Section

For the general 1-M section of Fig. 19, the Volterra response to a unit pulse $p(t) = u(t) - u(t-T)$ is obtained immediately from formulas (17) and (52). That is

$$y_2(t) =$$

$$\sum_{i,j,k=1}^{n} \frac{A_iB_jC_k}{a_ib_j}\left[d_o^{ijk} - d_1^{ijk}\, (\quad - d_2^{ijk}\, e^{-b_jt}\right.$$

$$\left. + d_3^{ijk}\, e^{-(a_i+b_j)t} + (d_4^{ijk} - d_5^{ijk})\, e^{-c_kt}\right] u(t)$$

$$\text{for } 0 \leq t < T$$

$$\sum_{i,j,k=1}^{n} \frac{A_iB_jC_k}{a_ib_j}\left[d_3^{ijk}(L^{ijk}-1)(M^{ijk}-1)e^{-(a_i+b_j)t'} + \right.$$

$$\left.((d_4^{ijk} - d_5^{ijk})N^{ijk} + d_5L^{ijk} + d_7M^{ijk} - d_5^{ijk} - d_6^{ijk})e^{-c_kt'}\right] u(t')$$

$$\text{for } T \leq t \qquad (53)$$

4.4.3 Symmetric 1-M Section

The counterparts of (52) and (53) for the symmetric case can be written immediately, but are not given for brevity.

Example 10

$$H_a(s) = H_b(s) = \frac{1}{s+1} - \frac{10}{s+5}$$

$$H_c(s) = \frac{4}{s+12}$$

Then using eq. 53 we have

$$V\{p_1,p_2\} =$$

$$\left\{ 4[\frac{1}{12} - \frac{1}{11}e^{-t} - \frac{1}{11}e^{-t} + \frac{1}{10}e^{-2t} + (\frac{1}{132} - \frac{1}{110})e^{-12t}] \right.$$

$$- \frac{40}{5}[\frac{1}{12} - \frac{1}{11}e^{-t} - \frac{1}{7}e^{-5t} + \frac{1}{6}e^{-6t} + (\frac{5}{84} - \frac{5}{66})e^{-12t}]$$

$$- \frac{40}{5}[\frac{1}{12} - \frac{1}{7}e^{-t} - \frac{1}{11}e^{-t} + \frac{1}{6}e^{-6t} + (\frac{1}{132} - \frac{1}{42})e^{-12t}]$$

$$\left. + \frac{400}{25}[\frac{1}{12} - \frac{1}{7}e^{-5t} - \frac{1}{7}e^{-5t} + \frac{1}{2}e^{-10t} + (\frac{5}{84} .. \frac{5}{14})e^{-12t}] \right\} u(t)$$

for $0 \leq t < 1$

$$\left\{ 4[\frac{1}{10}(e^{-1}-1)^2 e^{-2t'} + ((\frac{1}{132} - \frac{1}{110})e^{-12} + \frac{1}{110}e^{-1} + \frac{1}{110}e^{-1} - \frac{1}{110} \right.$$

$$\left. - \frac{1}{132})e^{-12t'}] \right.$$

$$- \frac{40}{5}[\frac{1}{6}(e^{-1}-1)(e^{-5}-1)e^{-6t'} + ((\frac{5}{84} - \frac{5}{66})e^{-12} + \frac{5}{66}e^{-1} + \frac{1}{42}e^{-5}$$

$$- \frac{5}{66} - \frac{1}{132})e^{-12}]$$

$$- \frac{40}{5}[\frac{1}{6}(e^{-1}-1)(e^{-5}-1)e^{-6t'} + ((\frac{1}{132} - \frac{1}{42})e^{-12} + \frac{1}{42}e^{-5}$$

$$+ \frac{5}{66}e^{-1} - \frac{1}{42} - \frac{5}{84})e^{-12t'}]$$

$$+ \frac{400}{25}[\frac{1}{2}(e^{-5}-1)^2 e^{-10t'} + ((\frac{5}{84} - \frac{5}{14})e^{-12} + \frac{5}{14}e^{-5}$$

$$\left. + \frac{5}{14}e^{-5} - \frac{5}{14} - \frac{5}{84})e^{-12}] \right\} u(t-1)$$

for $1 \leq t$

$$=$$

$$[0.3333 + 0.7273e^{-t} + 0.4000e^{-2t} - 2.285e^{-5t}$$
$$-2.6667e^{-6t} + 8.000e^{-10t} - 4.504e^{-12t}] \; u(t)$$

for $0 \leq t < 1$

$$[0.1598e^{-2(t-1)} - 1.6743e^{-6(t-1)} + 7.8926e^{-10(t-1)}$$
$$-5.7455e^{-12(t-1)}] \; u(t-1)$$

for $1 \leq t$

V. IDENTIFICATION OF $H_2(s_1,s_2)$ USING PULSE INPUTS

In this section we shall deal with the central problem of the report, i.e., identification of $H_2(s_1,s_2)$. It will be shown that this can be accomplished by use of either the bilinear response[3] to a pulse pair $p_1(t) = u(t) - u(t-T_1)$ and $p_2(t) = u(t-T_1) - u(t-T_1-T_2)$, or the Volterra response to a square pulse $p(t) = u(t) - u(t-T)$. It is assumed that the transfer function $H_2(s_1,s_2)$ is symmetric or, equivalently, that $H_a(s) = H_b(s)$ in the block diagram of (19). This assumption is entirely harmless because one can only identify the symmetric equivalent of a Volterra system from input-output measurements [7].

The problem is considered in two parts. First the estimation of poles of $H_a = H_b$ and H_c is considered. Next, the residues are estimated.

5.1 Identification of Poles

5.1.1 Poles from Bilinear Response

For a symmetric 1-M section the bilinear response to the square-pulse pair $p_1(t) = u(t) - u(t-T_1)$ and $p_2(t) = u(t) - u(t-T)$ was shown to be given by (47). Over the time interval $T_1 < t < T$ this response can be visualized as the step response of an equivalent linear system shown in Fig. 21, where $a_{ij} \triangleq a_i + a_j$ and the residues P_i, Q_{ij} and R_i are defined according to the second part of (47).

Clearly, the pencil-of-functions method[10],[12] can be used to find

a_i $\qquad i = 1, \ldots, n$

a_{ij} $\qquad j = 1, \ldots, i$

c_k $\qquad k = 1, \ldots, m$

Note that in general the total number of poles is

$$N = n + \frac{n(n+1)}{2} + m \tag{54}$$

If the 1-M section is completely symmetric, i.e., if $H_a = H_b = H_c$, then the total number of poles is again given by (54); however the poles a_i occur with a multiplicity of 2, i.e.,

$$c_k = a_k$$

[3] The reason for the interest in the bilinear response is the extra control on the energies of the various modes provided by the widths of the pulses p_1 and p_2.

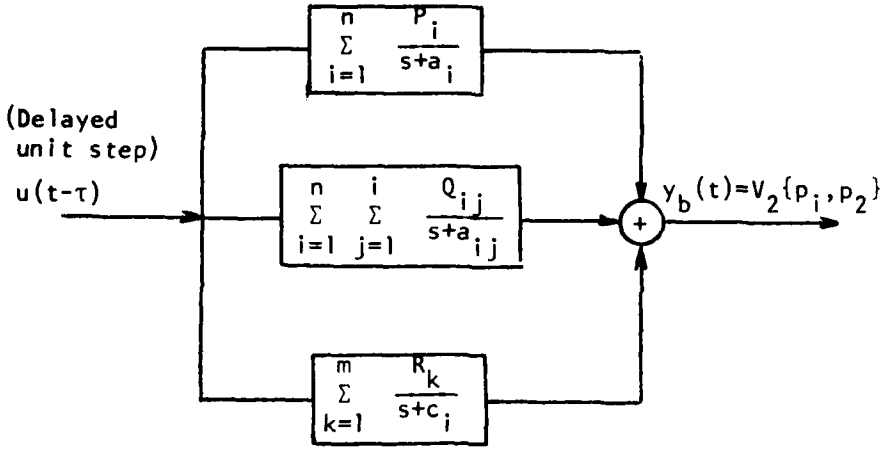

$$\tau = \begin{cases} T_1 & \text{for the response over } T_1 \leq t < T \\ T & \text{for the response over } T \leq t \end{cases}$$

Fig. 21 Equivalent linear system for bilinear response of $H_2(s_1,s_2)$

We remark that the type of $H_2(s_1,s_2)$ considered by Ewen were completely symmetric 1-M type. The simulation examples given below all pertain to completely symmetric 1-M sections.

Example 11

Consider a 1-M section with

$$H_a(s) = H_b(s) = H_c(s) = \frac{50.5}{s^2+s+25.25}$$

The bilinear response to square pulses p_1,p_2 with $T_1 = 1$ s. and $T_2 = 1$ s. (so that $T = 2$ s.) was generated over the interval $T_1 \leq t < T$.

Using a sampling interval $\Delta = 0.02$ s., the response was identified using the computer program IGRAM. The following s-domain poles were obtained

$s_1 = -0.553 - j5.023$

$s_2 = -0.553 + j5.023$

$s_3 = -1.135 + j4.9792$

$s_4 = -0.998 - j10.025$

$s_5 = -0.998 + j10.025$

$s_6 = -1.1396 - j9.9968$

$s_7 = -1.0021$

The normalized mean square error was $\nu = -0.0012$. Note that the following program parameters were used IREM = 0, IDLY = 0.

By observation it is deduced that

$a_1 = 0.553 + j5.023$

$a_2 = 0.553 - j5.023$

Over the time interval $T \leq t$ the bilinear response is given by the third part of (47), and can be visualized as the unit impulse response of a linear system as shown in Fig. 22.

Again the pencil-of-functions method can be applied to determine

a_{ij} $\quad i = 1, \ldots, n \quad j = 1, \ldots, i$

c_k $\quad k = 1, \ldots, m$

Note that the total number of poles is

$$N = \frac{n(n+1)}{2} + m \tag{55}$$

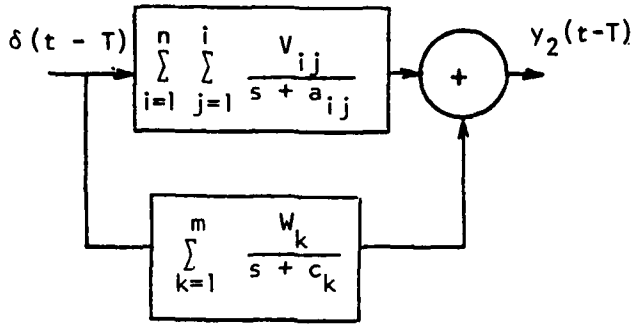

Fig. 22. Equivalent linear system for quadratic response of $H_2(s_1, s_2)$. Note that $a_{ij} = a_i + a_j$. Valid for $T \leq t$

5.1.2 Poles from Volterra Response

For a 1-M section the Volterra response to the square pulse $p(t) = u(t) - u(t-T)$ was shown to be given by the first part of (53). For the symmetric case this response can be shown to equal the step response of an equivalent linear system. This linear system has the same form as in Fig. 21 with $\tau = 0$. Recall that $a_{ij} = a_i + a_j$ and the residues are defined suitably.

Again, the pencil-of-functions method can be applied to determine

a_i $\quad i = 1, \ldots, n$

a_{ij} $\quad j = 1, .., i$

c_k $\quad k = 1, \ldots, m$

In general, the total number of poles is

$$N = n + \frac{n(n+1)}{2} + m \tag{56}$$

If the quadratic is <u>completely symmetric</u>, i.e., if $H_a = H_c$, then the total number of poles is again given by (56); however, the poles a_i occur with a multiplicity of 2.

Over the time interval $T \leq t$ the quadratic response is given by the second part of (53), and can be visualized as the unit impulse response of a linear system as shown in Fig. 22.

Again the pencil-of-functions method can be applied to determine

$$a_{ij} \qquad i = 1,\ldots,m \qquad j = 1,\ldots,i$$

$$c_k \qquad k = 1,\ldots,m$$

Note that the total number of poles is

$$N = \frac{n(n+1)}{2} + m \tag{57}$$

5.1.3 Remarks

1. The test engineer has a choice here between the use of the two segments of $y_b(t)$ (or $y_2(t)$). At this time it appears that the use of last segment is preferrable, since the dimensionality of identification is lower in this case (as evidenced from a comparison of (54) with (55)), although quite extensive experimentation is necessary to make a definitive statement.

2. Since the identified values $\hat{a}_{ij}$ and $\hat{c}_k$ will not coincide with the true values, it is necessary to isolate the poles by visual inspection or by a suitable computer routine. For example, if these numbers for the case $(n,m) = (2,1)$ are

2.1, 4.15, 9.8, 5.95

then

$$\hat{a}_{11} = 2.1$$

$$\hat{a}_{12} = 4.15$$

$$\hat{a}_{22} = 5.95$$

$$\hat{c}_1 = 9.8$$

and we may take

$$\hat{a}_1 = 1.05$$

$$\hat{a}_2 = 3.1$$

$$\hat{c}_1 = 9.8$$

5.2 Identification of Residues

After the poles have been determined, we can write

$$y_2(t) = \sum_{i=1}^{n} \sum_{j=1}^{i} \sum_{k=1}^{m} A_i A_j C_k \, f_{ijk}(t) \tag{58a}$$

where $f_{ijk}(t)$ are defined in accordance with (47) or (53) (these are known functions of the poles and the pulse width T). Further, by defining

$$e_\nu = A_i A_j C_k \qquad \nu = i + j + k - 2 \tag{58b}$$

$$g_\nu(\mu) = f_{ijk}(\mu\Delta) \qquad \mu = 0,\ldots,M-1 \tag{58c}$$

we obtain the following set of simultaneous equations[4]

$$\underline{Y} = G\,\underline{E} \tag{59}$$

where

$$\underline{Y} = [y_2(0)\ y_2(\Delta). \ldots .\ y_2((M-1)\Delta)]^T$$

$$G = [g_\nu(\mu)] \qquad M \times I \text{ matrix}$$

$$\underline{E} = [e_1 \ldots e_I]$$

Note that M denotes the number of time samples used in (58) and (59), and I denotes the number of unknown residue-products. If M is chosen equal

[4] If some of the poles are complex (occurring, in conjugate pairs), the associated residues are also complex. In such cases, it is possible to equate real (and imaginary) parts on both sides of the equation (59) to obtain real coefficient equations

to I then, we obtain the solution

$$\underline{E} = G^{-1} \underline{Y} \tag{60}$$

More generally if M > I, then we obtain the least-squares solution [15]

$$\underline{E} = (G^T G)^{-1} G^T \underline{Y} \tag{61}$$

Finally, the equations (58b) can be solved straightforwardly to yield the residues A_i and C_k. Because of the homogeneity of the relations any one of the real residues (or the magnitude of a complex residue) can be taken as 1.

VI. EXAMPLES

Two computer-generated examples will be presented. The first is a simple case with n=m=1 and is intended to clearly present the details of the procedure. The second is a more complicated case, representing a somewhat realistic channel. It has a linear transfer function characterized by a 6th order butterworth filter, and a quadratic transfer function with (m,n)=(3,1).

Example 12

Consider that the response $y_2(t)$ of a quadratic subsystem, with $H_a(s)=1/(s+1)$ and $H_b(s)=1/(s+0.5)$, to a square pulse of one second duration has been measured. With a sampling interval $\Delta = 0.02$, $q = 0.8$, and input a unit sample pulse (digital impulse), the symmetric Gram matrix of the information signals turns out to be (only lower triangular entries are shown)

$$\begin{bmatrix} 0.88303D+01 & & & & \\ 0.41058D+02 & 0.19507D+03 & & & \\ 0.18843D+03 & 0.90828D+03 & 0.42871D+04 & & \\ -0.16677D+01 & -0.46324D+01 & -0.12867D+02 & 0.27778D+01 & \\ -0.91383D+01 & -0.33616D+02 & -0.11623D+03 & 0.77160D+01 & 0.35151D+02 \end{bmatrix}$$

The normalized cofactor square-roots ($\sqrt{\bar{D}}_i/\sqrt{\bar{D}}_1$) are

1.0000 0.35933 0.032129 0.22357 0.026502

By use of (6) and (7b) the negatives of the poles are computed to be[5]

[5] The reason to associate 1.9997 with a_{11} is that when segment 1 is analyzed, a pole at 0.9996 also shows up.

$$a_{11} = 1.9997$$

$$c_1 = 0.5002$$

so that

$$a_1 = 0.9998$$

$$c_1 = 0.5002$$

Note that the waveform-fit error in modeling the poles was almost negligible (normalized mean-square error = 10^{-7}) pointing to the success of pulse testing approach.

Now, using these poles we find

$$y_2(t') = A_1A_1C_1\ (-0.2664375\ e^{-1.9997t'} + 0.4119195e^{-0.5002t'})$$

Using a single point, $y_2(t'=0) = 0.292924$, we obtain $A_1A_1C_1 = 2.013$, so that[6]

$$A_1 = 1$$

$$C_1 = 2.013$$

Example 13

Linear TF $H_1(s)$ Sixth order butterworth with cutoff $f_c = 10$ MHz

$$H_1(s) = \frac{6.1528908(10^{46})}{[s^6 + 2.4276(10^8)s^5 + 2.9467(10^{16})s^4 + 2.2676(10^{24})s^3 + 1.1633(10^{32})s^2 + 3.78358(10^{39})s + 6.1528908(10^{46})]}$$

$$\rightarrow \frac{6.1528908(10^{10})}{[\lambda^6 + 242.76\lambda^5 + 29467\lambda^4 + 2267581\lambda^3 + 1.6133(10^8)\lambda^2 + 3.78358(10^9)\lambda + 6.1528908(10^{10})]}$$

[6] A better value $A_1A_1C_1 = 2.0007$ is obtained using 50 points and formula (21).

Where $\lambda = (10^{-6})s$ (units of Mrad./s).

Quadratic TF $\quad H_a(s)=H_c(s)= \dfrac{50.5(10^{13})}{s^2 + (10^7)s + 25.25\ (10^{14})}$

$$= \frac{505}{\lambda^2 + 10\lambda + 2525}$$

The above 2-variable system was excited by a square pulse p(t) of duration T = 1 sec and the response $y^+(t)$ recorded. The system was next excited by the opposite polarity pulse -p(t) and the corresponding response $y^-(t)$ also recorded. From these responses we obtained[7] the linear response $y_1(t)$ and the quadratic response $y_2(t)$ by use of (11).

The results of identification are given below:

Estimated Linear Transfer Function -

$$\hat{H}(\lambda) = \frac{15.2\ \lambda\ + 6.1523(10^{10})}{[\lambda^6 + 242.76\lambda^5 + 29467\lambda^4 + 2267593\lambda^3 + 1.6133(10^8)\lambda^2 + 3.784(10^9)\lambda + 6.15237(10^{10})\ ]}$$

Estimated Quadratic Transfer Function

$$\hat{H}_a(\lambda)= \hat{H}_c(\lambda)= \frac{0.003\ \lambda + \ 505.07}{\lambda^2 + 9.9998\lambda + 2524.8}$$

[7] It is easy to show that $y_1(t) = \frac{1}{2}[y^+(t) - y^-(t)]$, and $y_2(t)= \frac{1}{2}[y^+(t)+y^-(t)]$.

REFERENCES

[1] V. Volterra, Theory of Functionals and of Integral and Integro-Differential Equations. Dover Publications, New York, 1959.

[2] N. Wiener, Nonlinear Problems in Random Theory. The Technology Press, M.T.T., and John Wiley, New York, 1958.

[3] Y. H. Ku and A. A. Wolfe, "Volterra-Wiener functionals for the analysis of nonlinear systems," J. Franklin Institute, Vol. 281, pp. 9-26, January 1966.

[4] S. Narayanan, "Application of Volterra series to intermodulation distortion analysis of transistor feedback amplifiers," IEEE Trans. Circuit Theory, Vol. CT-17, pp. 518-523, November 1970.

[5] J. Goldman, "A Volterra series description of crosstalk interference in communication systems," Bell System Technical Journal, Vol. 52, pp. 649-688, May 1973.

[6] K. Y. Chang, "Intermodulation noise and products due to frequency dependent nonlinearities in CATV systems," IEEE Trans. Comm., Vol. COM-23, January 1975.

[7] M. Schetzen, The Volterra and Wiener Theories of Nonlinear Systems. John Wiley, New York, 1979.

[8] E. J. Ewen, "Black-box identification of nonlinear Volterra Systems," Ph.D. Dissertation, Syracuse University, December 1975.

[9] V. K. Jain, "On system identification and approximation," Research Report SS-I1, Florida State University, 1970.

[10] V. K. Jain, "Advanced technique for blackbox modeling," Rome Air Development Center Technical Report, RADC-TR-80-343, 1980. (A094731)

[11] V. K. Jain, "Representation of sequences," IEEE Trans. Audio and Electroacoustics," Vol. AU-19, pp. 515-523, September 1971.

[12] V. K. Jain, "Filter analysis by use of pencil-of-functions," IEEE Trans. Circuits and Systems, Vol. CAS-21, pp. 574-583, September 1974.

[13] W. D. Stanley, Digital Signal Processing. Reston (Prentice-Hall), Reston, 1975.

[14] A. M. Bush, "Some Techniques for the Synthesis of Nonlinear Systems," Sc.D. Thesis, Dept. of Electrical Engineering, M.I.T., 1965

[15] C. R. Rao and S. K. Mitra, Generalized Inverse of Matrices, and Applications. New York, Wiley, 1971.

APPENDIX A

GEORGE'S THEOREM

This theorem helps evaluation of the quadratic volterra response (or the bilinear response) by inspection from the associated response.

Theorem If

$$Y_{(2)}(s_1,s_2) = \frac{1}{(s_1+a)(s_2+b)}\, C(s_1+s_2) \tag{B1}$$

then

$$Y_2(s) = \frac{C(s)}{s+a+b} \tag{B2}$$

Proof: It is readily shown that

$$Y_2(s) = \frac{1}{2\pi j} \int_{-j\infty}^{j\infty} \frac{C(s)}{(s_1+a)(s-s_1+b)}\, ds_1 \tag{B3}$$

(see Schetzen [7]). Then the desired result follows immediately by use of the residue theorem.

Corollary Let

$$\bar{Y}_2\ (s_1,s_2) = \frac{e^{-\alpha s_1} e^{-\beta s_2}}{(s_1+a)(s_2+b)}\, C(s) \tag{B4}$$

If $\beta > \alpha$, then

$$Y_2(s) = e^{-a(\beta-\alpha)}\, \frac{e^{-\beta s} C(s)}{(s+a+b)} \tag{B5}$$

If $\alpha > \beta$ then

$$Y_2(s) = e^{-b(\alpha-\beta)}\, \frac{e^{-\alpha s} C(s)}{(s+a+b)} \tag{B6}$$

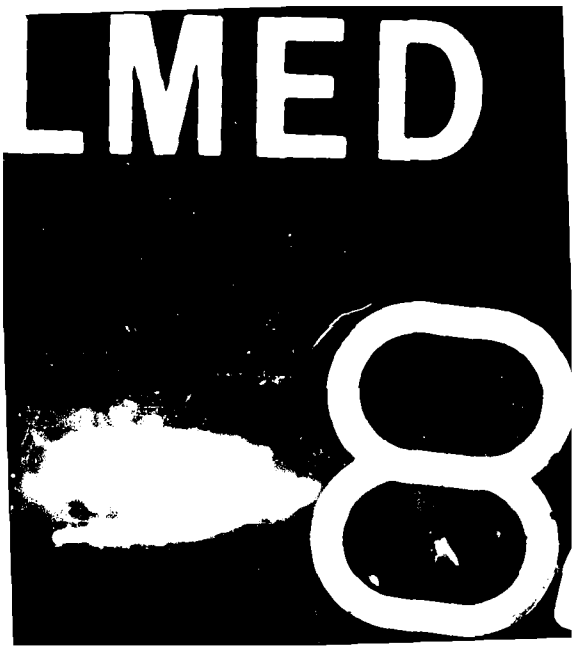
LMED
8